



**PWROG-20025-NP**  
**Revision 0**

WESTINGHOUSE NON-PROPRIETARY CLASS 3

# **Methodology for Adjusting Reactor Pressure Vessel Embrittlement Predictions using Heat-Specific Surveillance Data**

**Materials Committee**

**PA-MS-C-1759**

October 2020



**Westinghouse**

**framatome**

**PWROG-20025-NP**  
**Revision 0**

# **Methodology for Adjusting Reactor Pressure Vessel Embrittlement Predictions using Heat-Specific Surveillance Data**

**PA-MS-C-1759**

**J. Brian Hall\***  
Churchill Laboratory Services

**October 2020**

Reviewer: Benjamin E. Mays\*  
License Renewal, Radiation Analysis, & Nuclear Operations

Approved: David B. Love\*, Manager  
Churchill Laboratory Services

Approved: James P. Molkenhuth\*, Program Director  
PWR Owners Group PMO

\*Electronically approved records are authenticated in the electronic document management system.

---

Westinghouse Electric Company LLC  
1000 Westinghouse Drive  
Cranberry Township, PA 16066, USA

© 2020 Westinghouse Electric Company LLC  
All Rights Reserved

## ACKNOWLEDGEMENTS

This report was developed and funded by the PWR Owners Group under the leadership of the participating utility representatives of the Materials Committee. The author would like to thank the following people and/or organizations for their valuable contributions to this report:

Matt DeVan – Framatome, Inc.

Mark Kirk – Phoenix Engineering Associates, Inc.

Scott Sidener – Westinghouse

Brett Lynch - Westinghouse

### LEGAL NOTICE

This report was prepared as an account of work performed by Westinghouse Electric Company LLC. Neither Westinghouse Electric Company LLC, nor any person acting on its behalf:

1. Makes any warranty or representation, express or implied including the warranties of fitness for a particular purpose or merchantability, with respect to the accuracy, completeness, or usefulness of the information contained in this report, or that the use of any information, apparatus, method, or process disclosed in this report may not infringe privately owned rights; or
2. Assumes any liabilities with respect to the use of, or for damages resulting from the use of, any information, apparatus, method, or process disclosed in this report.

### COPYRIGHT NOTICE

This report has been prepared by Westinghouse Electric Company LLC and bears a Westinghouse Electric Company copyright notice. As a member of the PWR Owners Group, you are permitted to copy and redistribute all or portions of the report within your organization; however all copies made by you must include the copyright notice in all instances.

### DISTRIBUTION NOTICE

This report was prepared for the PWR Owners Group. This Distribution Notice is intended to establish guidance for access to this information. This report (including proprietary and non-proprietary versions) is not to be provided to any individual or organization outside of the PWR Owners Group program participants without prior written approval of the PWR Owners Group Program Management Office. However, prior written approval is not required for program participants to provide copies of Class 3 Non-Proprietary reports to third parties that are supporting implementation at their plant, and for submittals to the NRC.

**PWR Owners Group  
United States Member Participation\* for PA-MS-C-1759**

Utility Member	Plant Site(s)	Participant	
		Yes	No
Ameren Missouri	Callaway (W)	X	
American Electric Power	D.C. Cook 1 & 2 (W)	X	
Arizona Public Service	Palo Verde Unit 1, 2, & 3 (CE)	X	
Dominion Energy	Millstone 2 (CE)	X	
	Millstone 3 (W)	X	
	North Anna 1 & 2 (W)	X	
	Surry 1 & 2 (W)	X	
	V.C. Summer (W)	X	
Duke Energy Carolinas	Catawba 1 & 2 (W)	X	
	McGuire 1 & 2 (W)	X	
	Oconee 1, 2, & 3 (B&W)	X	
Duke Energy Progress	Robinson 2 (W)	X	
	Shearon Harris (W)	X	
Entergy Palisades	Palisades (CE)		X
Entergy Nuclear Northeast	Indian Point 2 & 3 (W)		X
Entergy Operations South	Arkansas 1 (B&W)	X	
	Arkansas 2 (CE)	X	
	Waterford 3 (CE)	X	
Exelon Generation Co. LLC	Braidwood 1 & 2 (W)	X	
	Byron 1 & 2 (W)	X	
	Calvert Cliffs 1 & 2 (CE)	X	
	Ginna (W)	X	
Energy Harbor	Beaver Valley 1 & 2 (W)	X	
	Davis-Besse (B&W)	X	
Florida Power & Light \ NextEra	St. Lucie 1 & 2 (CE)	X	
	Turkey Point 3 & 4 (W)	X	
	Seabrook (W)	X	
	Pt. Beach 1 & 2 (W)	X	
Luminant Power	Comanche Peak 1 & 2 (W)	X	

**PWR Owners Group  
United States Member Participation\* for PA-MS-C-1759**

Utility Member	Plant Site(s)	Participant	
		Yes	No
Pacific Gas & Electric	Diablo Canyon 1 & 2 (W)		X
PSEG – Nuclear	Salem 1 & 2 (W)	X	
So. Texas Project Nuclear Operating Co.	South Texas Project 1 & 2 (W)	X	
Southern Nuclear Operating Co.	Farley 1 & 2 (W)	X	
	Vogtle 1 & 2 (W)	X	
Tennessee Valley Authority	Sequoyah 1 & 2 (W)	X	
	Watts Bar 1 & 2 (W)	X	
Wolf Creek Nuclear Operating Co.	Wolf Creek (W)	X	
Xcel Energy	Prairie Island 1 & 2 (W)	X	

\* **Project participants as of the date the final deliverable was completed. On occasion, additional members will join a project. Please contact the PWR Owners Group Program Management Office to verify participation before sending this document to participants not listed above.**

**PWR Owners Group  
International Member Participation\* for PA-MS-C-1759**

Utility Member	Plant Site(s)	Participant	
		Yes	No
AXPO AG	Beznau 1 & 2 (W)	X	
Asociación Nuclear Ascó-Vandellòs	Asco 1 & 2 (W)	X	
	Vandellos 2 (W)	X	
Centrales Nucleares Almaraz-Trillo	Almaraz 1 & 2 (W)	X	
EDF Energy	Sizewell B (W)	X	
Electrabel	Doel 1, 2 & 4 (W)	X	
	Tihange 1 & 3 (W)	X	
Electricite de France	58 Units	X	
Elektricitets Produktiemaatschappij Zuid-Nederland	Borssele 1 (Siemens)	X	
Eletronuclear-Eletrabras	Angra 1 (W)	X	
Emirates Nuclear Energy Corporation	Barakah 1 & 2	X	
Hokkaido	Tomari 1, 2 & 3 (MHI)	X	
Japan Atomic Power Company	Tsuruga 2 (MHI)	X	
Kansai Electric Co., LTD	Mihama 3 (W)	X	
	Ohi 3 & 4 (MHI)	X	
	Takahama 1, 2, 3 & 4 (W & MHI)	X	
Korea Hydro & Nuclear Power Corp.	Kori 1, 2, 3 & 4 (W)	X	
	Hanbit 1 & 2 (W)	X	
	Hanbit 3, 4, 5 & 6 (CE)	X	
	Hanul 3, 4, 5 & 6 (CE)	X	
Kyushu	Genkai 2, 3 & 4 (MHI)	X	
	Sendai 1 & 2 (MHI)	X	
Nuklearna Elektrarna KRSKO	Krsko (W)	X	
Ringhals AB	Ringhals 3 & 4 (W)	X	
Shikoku	Ikata 3 (MHI)	X	
Taiwan Power Co.	Maanshan 1 & 2 (W)	X	

\* **Project participants as of the date the final deliverable was completed. On occasion, additional members will join a project. Please contact the PWR Owners Group Program Management Office to verify participation before sending this document to participants not listed above.**

## TABLE OF CONTENTS

LIST OF TABLES .....	ix
LIST OF FIGURES .....	x
1 INTRODUCTION.....	1-1
2 METHODOLOGY DESCRIPTION FOR MEASURED SURVEILLANCE HEATS .....	2-1
2.1 ZERO TO ONE CAPSULE .....	2-3
2.2 TWO TO FOUR CAPSULES.....	2-3
2.2.1 Bias Adjustment Procedure for 2-4 Capsules .....	2-4
2.3 FIVE OR MORE CAPSULES .....	2-5
2.3.1 Bias and Slope Adjustment Procedure for Five or More Capsules .....	2-5
2.4 LIMITS OF APPLICABILITY .....	2-7
3 EXAMPLE APPLICATIONS OF METHODOLOGY .....	3-1
3.1 INTERMEDIATE SHELL FORGING .....	3-1
3.2 PLATE HEAT B6903.....	3-4
3.3 WELD HEAT 895075.....	3-8
4 METHOD DEVELOPMENT .....	4-1
4.1 EMBRITTLEMENT SHIFT .....	4-1
4.2 UNCERTAINTY DETERMINATION.....	4-2
4.3 DERIVATION OF UNCERTAINTY TERMS .....	4-3
4.3.1 Determination of Weld Uncertainty Terms .....	4-4
4.3.2 Determination of Forging Uncertainty Terms .....	4-5
4.3.3 Determination of Plate Uncertainty Terms .....	4-6
4.3.4 Standard Reference Material Plate Uncertainty Terms.....	4-8
4.3.5 Uncertainty Determination for Multiple RPVs .....	4-10
5 REFERENCES.....	5-1
APPENDIX A METHODS CONSIDERED .....	A-1



## LIST OF TABLES

Table 2-1	Summary of Key Calculational Parameters Based on Number of Tested Capsules .....	2-2
Table 2-2	Values of $\sigma_{heat}$ .....	2-2
Table 2-3	Coefficients for E900-15 SD Equation .....	2-3
Table 2-4	Uncertainty of TTS Bias and Adjustment Limit by Product Form.....	2-4
Table 3-1	Intermediate Shell Forging Best Estimate Chemistry (#1).....	3-1
Table 3-2	Intermediate Shell Forging TTS Data .....	3-1
Table 3-3	Plate Heat B6903 Best Estimate Chemistry and Projected RPV Temperature (#1 and #3) .....	3-4
Table 3-4	Plate Heat B6903 TTS Data .....	3-5
Table 3-5	Weld Heat 895075 Hypothetical RPV Chemistry (#3) .....	3-8
Table 3-6	Weld Heat 895075 TTS Data .....	3-9
Table 4-1	Plate Statistics .....	4-7
Table 4-2	SRM Uncertainty .....	4-8

## LIST OF FIGURES

Figure 3-1	Intermediate Shell Forging E900-15 Prediction Compared to Measured TTS ...	3-3
Figure 3-2	Intermediate Shell Forging E900-15 Adjusted Prediction Compared to Measured TTS #5.....	3-3
Figure 3-3	Plate Heat B6903 E900-15 Prediction Compared to Measured TTS .....	3-7
Figure 3-4	Plate Heat B6903 E900-15 Adjusted Prediction Compared to Measured TTS ..	3-7
Figure 3-5	Weld Heat 895075 E900-15 Prediction Compared to Measured TTS.....	3-13
Figure 3-6	Weld Heat 895075 E900-15 Adjusted Prediction Compared to Measured TTS .....	3-13
Figure 4-1	Weld Error-Adjusted Residuals Compared to Twice $\sigma_{\text{heat}}$ for Welds.....	4-5
Figure 4-2	Forging Error-Adjusted Residuals Compared to Twice $\sigma_{\text{heat}}$ for Forgings .....	4-6
Figure 4-3	Error-Adjusted Residuals Compared to Twice $\sigma_{\text{heat}}$ for Higher Ni Plates.....	4-8
Figure 4-4	Plate Heat-specific $\sigma$ versus Sample Size .....	4-9
Figure 4-5	Error-Adjusted Residuals Compared to Twice $\sigma_{\text{heat}}$ for SRM Plates.....	4-10

# 1 INTRODUCTION

This report provides a method for adjusting Reactor Pressure Vessel (RPV) embrittlement predictions and crediting increased knowledge when considering measured heat-specific surveillance data. This method is intended to be incorporated into Section 2500 of the proposed ASME Section XI Code Case, titled “Accounting for the Effects of Neutron Irradiation Embrittlement in Flaw Evaluations of Pressure Boundary Materials in Class 1 Ferritic Steel Components Section XI, Division 1” [1]. The method draws on the Westinghouse and Framatome extensive practical experience in applying credibility evaluations to surveillance data to ensure that the method is practical, useful, and technically robust. The method is designed to be used with ASME Section XI, Appendix G pressure-temperature heatup and cooldown curves [2] and as a possible replacement for portions of Regulatory Guide 1.99, Revision 2 [3] and 10 CFR 50.61 [4]. The method has been developed using ASTM Standard Guide E900-15 [5] which is the most recent internationally accepted consensus standard for predicting RPV embrittlement. In addition, the uncertainty terms were developed using the same large international database used to develop E900-15, therefore it can be applied to any ASME, or similar, specification RPV steel within the limitations of E900-15.

This report is part of the effort to provide a method for accounting for the effect of neutron irradiation embrittlement on RPV steels which the ASME Code does not currently address. In the U.S., methods to account for irradiation embrittlement have been provided in Regulatory Guide 1.99, Revision 2 [3] and 10 CFR 50.61 [4]. These methods are dated and suffer from a number of inadequacies [6]. Section 2 of this report describes the methodology and the detailed steps in its application when assessing measured surveillance data for a specific heat. Section 3 gives examples of how the method is applied. Section 4 provides the reasoning and technical basis for the developed method. Appendix A briefly describes other methods that were considered in the development of this methodology, but not selected.

## 2 METHODOLOGY DESCRIPTION FOR MEASURED SURVEILLANCE HEATS

The equation used to calculate the ductile-brittle transition region adjusted reference temperature (ART) is shown as Equation 1.

$$\text{Equation 1} \quad \text{ART} = \text{RT}_u + \Delta\text{RT} + 2\sqrt{\sigma_u^2 + \sigma_\Delta^2}$$

Where,

$\text{RT}_u$  = unirradiated reference temperature

$\Delta\text{RT}$  = reference temperature shift due to irradiation, defined in Equation 2

$\sigma_u$  = uncertainty (standard deviation) of  $\text{RT}_u$

$\sigma_\Delta$  = uncertainty (standard deviation) of  $\Delta\text{RT}$ , defined in Table 2-1

$\text{RT}_u$  and  $\sigma_u$  are not addressed herein, although the practice of using  $\sigma_u = 0^\circ\text{F}$  for measured values of  $\text{RT}_{\text{NDT}}$  per ASME NB-2300 is acceptable since  $\text{RT}_{\text{NDT}}$  is generally considered a bounding measure of transition temperature.

$$\text{Equation 2} \quad \Delta\text{RT} = \text{slope adjustment} \cdot \text{TTS} + \text{bias}$$

Where,

*Slope adjustment* is defined per Table 2-1

*TTS* = Transition Temperature Shift determined per the applicable Embrittlement Trend Correlation (ETC). For this report, the ETC utilized is that defined in ASTM E900-15.

*Bias* is defined per Table 2-1

Table 2-1 provides a summary of slope adjustment, bias, and  $\sigma_\Delta$  values, while Sections 2.1 through 2.3 provide specific details on how to apply this methodology depending on the number of heat-specific surveillance capsule measurements.

	Fluence of Prediction ≤ Fluence of Highest Measured Shift			Fluence of Prediction > Fluence of Highest Measured Shift		
Number of Tested Capsules <sup>(1)</sup>	Bias <sup>(2)</sup>	Slope Adjustment <sup>(2)</sup>	$\sigma_{\Delta}$	Bias <sup>(2)</sup>	Slope Adjustment <sup>(2)</sup>	$\sigma_{\Delta}$
0-1	0	1	$SD_{ETC}$	0	1	$SD_{ETC}$
2-4	Average	1	$\sqrt{\sigma_{heat}^2 + \sigma_{multiplant}^2}$	Average	1	$SD_{ETC}$
≥ 5	Best-fit	Best-fit	$\sqrt{\sigma_{heat}^2 + \sigma_{multiplant}^2}$	Best-fit	Best-fit with slope ≥ 1.0 <sup>(3)</sup>	$SD_{ETC}$

Notes:

- (1) This number represents the number of capsules that have been tested which contain the material, not the number of total datasets from the capsules. Thus, a capsule containing both strong-direction and weak-direction data is only considered one capsule for the purposes of this table.
- (2) Detailed calculation procedures and limits on the “Average” and “Best-fit” parameters are described in detail in Sections 2.2.1 and 2.3.1, respectively.
- (3) For adjusted slopes determined to be less than one, the slope must be increased to one when predicting above the fluence of the highest measured shift. This adjustment is described in detail in Section 2.3.1.

$\sigma_{heat}$  = the uncertainty of the  $\Delta RT$  prediction based on the heat-specific measured data from the plant of interest.  $\sigma_{heat}$  is summarized in Table 2-2 and derived in Section 4.2 and Section 4.3.

$\sigma_{multiplant}$  = the added uncertainty if surveillance data was irradiated in plant(s) other than the plant to which the data is being applied. If data from another plant is being applied,  $\sigma_{multiplant} = 11^{\circ}F$  (derived in Section 4.3), otherwise  $\sigma_{multiplant} = 0^{\circ}F$ .

Product Form	$\sigma_{heat}$ (°F)
Weld	16.9
Forging	16.4
A-533B & A-302BM Plate	13.3
A-302B Plate	N/A, $\sigma_{\Delta} = SD_{ETC}$

$SD_{ETC}$  = the uncertainty (standard deviation) determined by the applicable ETC. For this report, the ASTM E900-15 ETC is utilized. The equation for the E900-15  $SD_{ETC}$  is summarized in Equation 3.

**Equation 3**  $SD_{ETC} = C \cdot TTS^D$

Where,

TTS = E900-15 predicted shift in 30 ft-lb transition temperature (°C)

C and D are provided in Table 2-3:

<b>Product Form</b>	<b>C</b>	<b>D</b>
Forgings	6.972	0.199
Plates and Standard Reference Material (SRM) Plates	6.593	0.163
Welds	7.681	0.181

## 2.1 ZERO TO ONE CAPSULE

If zero or only one measured TTS irradiation condition is available for a specific heat, then there is insufficient data to make adjustments and the ETC (in this case E900-15) should be used with its associated  $\sigma$  for making embrittlement predictions. Note that two measurements from one capsule for the same heat (e.g. two orientations) is only considered one irradiation condition. Best-estimate values of the ETC inputs should be used for the heat. The inputs to Equation 1 are as follows:

$$\Delta RT = TTS \text{ from E900-15 (i.e., slope adjustment} = 1 \text{ and bias} = 0 \text{ for Equation 2)}$$

$$\sigma_{\Delta} = SD_{ETC} \text{ per Equation 3}$$

## 2.2 TWO TO FOUR CAPSULES

Measurement data from 2-4 capsules provides sufficient data that the heat-specific bias relative to the ETC prediction can be corrected with a bias term. However, the slope adjustment is not used (i.e., *slope adjustment* is set to a value of 1).

The knowledge of the heat-specific measurements provides more certainty and the inability of the ETC to predict differences between heats can be eliminated. Therefore, the  $\sigma_{\Delta}$  from the ETC can be reduced to  $\sigma_{heat}$  summarized in Table 2-2 if the fluence being analyzed is within the range of the surveillance capsule data and only plant-specific data is being considered. If the data includes measurements from a different plant,  $\sigma_{multiplant}$  must also be considered. Since  $\sigma_{heat}$  and  $\sigma_{multiplant}$  are independent, determination of  $\sigma_{\Delta}$  is based on the square root of the sum of the squares of these values as shown in Table 2-1. For the purposes of this report the capsule fluence “range” is considered to be from  $10^{17}$  n/cm<sup>2</sup> (or lower if a lower fluence capsule is available) to the highest fluence capsule’s fluence value. A cut-off of  $10^{17}$  n/cm<sup>2</sup> was selected as below this fluence, shift is considered to be zero. If the fluence being analyzed is above the highest fluence capsule’s fluence,  $\sigma_{\Delta} = SD_{ETC}$  must be utilized.

### 2.2.1 Bias Adjustment Procedure for 2-4 Capsules

In order to adjust the ETC prediction for heat-specific data bias, use the following procedure:

1. Gather surveillance data for the heat of interest. The data to be gathered includes measured TTS and input values (fluence, chemistry, temperature, etc.) for each data point. All data should be included that came from specimens irradiated in a power reactor within the limits of applicability of the ETC. Measured TTS values less than zero should conservatively be set to zero.
2. Calculate the ETC prediction for each TTS measurement based on the material source chemistry best-estimate, time-weighted average irradiation temperature, and fluence best-estimate value for each measured TTS data point.
3. Determine the error of each ETC prediction by subtracting the ETC prediction (#2) from the measured TTS (#1).
4. Determine the average error of the ETC prediction by averaging each error determined in #3. This value is considered the heat-specific average bias.
5. Add the average bias term to the ETC prediction when making predictions for this heat in an RPV.

The bias should be limited to twice  $\sigma_{bias}$  for each product form as shown in Table 2-4. These values were developed as presented Section 4.3 and represent the standard deviation of the mean biases for a database of many heats from each product form. The limit is two times  $\sigma_{bias}$  because there is a 95% confidence that bias adjustments should be within this range. Biases which are calculated to be greater than the limit should be investigated to determine the cause (e.g., outlier or error in a data point), and the cause should be addressed if possible. If no cause can be found, the bias limit should be used. In addition, conservatively the shift prediction cannot be less than zero.

<b>Product</b>	<b><math>\sigma_{bias}</math> (°F)</b>	<b>Bias Limit (°F)</b>
Welds	23.7	47.4
Forgings	18.9	37.8
Plates	16.8	33.6

## 2.3 FIVE OR MORE CAPSULES

Measurement data from five or more capsules provides sufficient data that the heat-specific bias and slope difference from the ETC can be corrected using the slope adjustment in addition to the average bias correction. The knowledge of the added heat-specific measurements provides more certainty so that fluence trend deviation from the ETC can be corrected. Adjusting the slope and bias reduces residuals more than correcting for bias alone. As a result, the uncertainty is reduced. However, to be conservative, the  $\sigma_{heat}$  values from Table 2-2 should continue to be used. Thus,  $\sigma_{\Delta}$  can be set to the values in Table 2-2 if the fluence being analyzed is within the range of the surveillance capsule measured data and only plant-specific data is being considered. If the data includes measurements from a different plant,  $\sigma_{multiplant}$  must also be considered. Since  $\sigma_{heat}$  and  $\sigma_{multiplant}$  are independent, determination of  $\sigma_{\Delta}$  is based on the square root of the sum of the squares of these values as shown in Table 2-1. For the purposes of this report, the capsule fluence “range” is considered to be from  $10^{17}$  n/cm<sup>2</sup> (or lower if a lower fluence capsule is available) to the highest fluence capsule’s fluence value. A cut-off of  $10^{17}$  n/cm<sup>2</sup> was selected, as below this fluence shift is considered to be zero. If the fluence being analyzed is above this range,  $\sigma_{\Delta} = SD_{ETC}$  must be utilized.

### 2.3.1 Bias and Slope Adjustment Procedure for Five or More Capsules

1. Gather all surveillance data for the heat of interest. The data to be gathered includes measured TTS and input values to the ETC (fluence, chemistry, temperature, etc.) for each data point. All data should be included that came from specimens irradiated in a power reactor within the limits of applicability of the ETC. Measured TTS values less than zero should conservatively be set to zero.
2. Calculate the ETC prediction for each TTS measurement based on the best-estimate values (material source chemistry, average irradiation temperature and fluence) for each measured TTS data point.
3. Gather each of the best-estimate input parameters for the RPV material of interest (e.g., average projected irradiation temperature through end-of-life, best-estimate chemistry and fluence)
4. Calculate the ETC prediction using the best-estimate RPV input values (from #3) at the fluence of each measured TTS data point.
5. Determine the difference between the ETC prediction using the RPV material input values (#4) and the ETC prediction using values for the measured TTS material data points (#2).
6. Adjust measured TTS values (from #1) by the difference between the ETC prediction using the RPV material input values and the ETC prediction using values for the measured TTS material data point (from #5). In other words, adjust measured TTS from #1 by the adjustment determined in #5. If any values are less than 0°F, they should conservatively be set to 0°F.



7. Determine “best-fit” TTS prediction parameters from Equation 2 (slope adjustment and bias) using minimization of the mean square error. An example of how to complete this determination is described in detail below.
  - a. For each data point, create a “best-fit” TTS prediction equal to the ETC prediction from #4 times a slope adjustment of one and a bias of zero.
  - b. Calculate the residual error for each data point using the “best-fit” TTS prediction (the “best-fit” TTS prediction [#7a] minus the adjusted measured TTS values [#6]).
  - c. Square the errors calculated in #7b.
  - d. Sum the squared errors calculated in #7c.
  - e. Using Microsoft® Excel®<sup>1</sup> spreadsheet software “Solver” or a similar function, minimize the squared error sum (#7d) by changing the slope adjustment and bias values. The slope adjustment and bias value corresponding to the minimum squared error sum are considered the “best-fit” parameters. Note that bias values are limited by Table 2-4.
8. Use Equation 2 and the “best-fit” parameters from #7 to make TTS predictions for the RPV material of interest within the fluence range of the surveillance capsule data. If TTS predictions are made outside of the fluence range of the surveillance data when the best-fit slope is calculated to be less than 1, Equation 4 must be used instead of Equation 2.

**Equation 4**, If prediction fluence > highest capsule fluence and *slope adjustment* < 1.0

$$\Delta RT = TTS + (\textit{slope adjustment} - 1) \cdot TTS_{\textit{highestfluence}} + \textit{bias}$$

Where,

*Slope adjustment* is the best-fit determined per the procedure in 2.3.1

*TTS* = Transition Temperature Shift determined per the applicable ETC. For this report, the ETC utilized is that defined in ASTM E900-15.

*TTS<sub>highestfluence</sub>* = Transition Temperature Shift determined per the applicable ETC at the fluence of the highest fluence capsule.

*Bias* is the best-fit determined per the procedure in 2.3.1

---

<sup>1</sup> *Microsoft and Excel are either registered trademarks or trademarks of Microsoft Corporation in the United States and/or other countries*

To be conservative, only slope adjustments  $\geq 1$  can be used above the highest measured shift, which is ensured by the use of Equation 4. In effect, Equation 4 determines the best-fit TTS prediction at the maximum surveillance capsule fluence, then it adds the difference between what the unadjusted ETC predicts for the fluence of interest and the maximum capsule fluence.

## 2.4 LIMITS OF APPLICABILITY

This method is applicable to surveillance programs which meet the requirements of ASTM E185 (any year) [7] or supplemental surveillance capsules for material heats irradiated in PWR or BWRs with input variables in the ranges described below.

The application of this method is limited to chemistry values, average irradiation temperature, and fluence ranges from the database used to establish the ETC in E900-15 [5] since the E900-15 database (named "PLOTTER") [8] was used to establish the uncertainty values derived herein. The values for each of the inputs should be used with limits stated in the E900-15 (reproduced below). The methods herein can be used outside of this range if further justification is provided.

- Copper content up to 0.4%.
- Nickel content up to 1.7%.
- Phosphorus content up to 0.03%.
- Manganese content within the range from 0.55% to 2.0%.
- Irradiation temperature within the range from 255°C to 300°C (491°F to 572°F).
- Neutron fluence within the range from  $1 \times 10^{17}$  n/cm<sup>2</sup> to  $2 \times 10^{20}$  n/cm<sup>2</sup> ( $E > 1$  MeV).
- A categorical variable describing the product form (that is, weld, plate, forging).
- A-533 Type B Class 1 and 2, A-302 Grade B, A-302 Grade B (modified), and A-508 Class 2 and 3. Also, European and Japanese steel grades that are equivalent to these ASME/ASTM grades.
- Submerged arc welds, shielded arc welds, and electroslag welds having compositions consistent with those of the welds used to join the base materials described above.
- Neutron fluence rate within the range from  $3 \times 10^8$  n/cm<sup>2</sup>/s to  $5 \times 10^{12}$  n/cm<sup>2</sup>/s ( $E > 1$  MeV).
- Neutron energy spectra within the range expected at the reactor vessel region adjacent to the core of commercial PWRs and BWRs (greater than approximately 500MW electric).
- Additionally, scatter in the plots of Charpy energy versus temperature for the irradiated and unirradiated conditions should be small enough to permit the determination of the 30 ft-lb temperature unambiguously.

Note that embrittlement TTS with fluence less than  $1 \times 10^{17}$  n/cm<sup>2</sup> is considered to be indistinguishable from data scatter, and therefore, can be considered zero consistent with Regulatory Issue Summary (RIS) 2014-11 [9] and TLR-RES/DE/CIB-2013-01 [10].

### 3 EXAMPLE APPLICATIONS OF METHODOLOGY

This section presents a few example applications of the methodology detailed in Section 2. An example of applying the bias correction only (Section 3.1), an example including the bias and slope correction (Section 3.2), and a weld heat irradiated in multiple plants are included (Section 3.3).

#### 3.1 INTERMEDIATE SHELL FORGING

An example is presented for an actual PWR intermediate shell forging which was irradiated in three capsules. The data is taken primarily from [11] with updates to certain values based on later analyses. Since the number of capsules is between 2 and 4, the Section 2.2 method is used. The best estimate chemistry is presented in Table 3-1 and the measured and predicted TTS results are presented in Table 3-2. Step numbers from Section 2.2.1 are preceded by “#”.

<b>Element</b>	<b>Weight %</b>
Cu	0.086
Ni	0.86
P	0.014
Mn	0.73

<b>Capsule</b>	<b>Fluence (E &gt; 1 MeV)</b>	<b>Irradiation Temperature (°F)</b>	<b>Measured TTS (°F) #1</b>	<b>E900-15 Predicted TTS (°F) #2</b>	<b>Residual (°F) #3</b>
Z – Tang.	2.86E+18	562	0 <sup>(1)</sup>	26.4	-26.4
Y – Tang.	1.29E+19	562	19.09	47.2	-28.1
V – Tang.	2.27E+19	562	25.61	58.1	-32.5
Z – Axial	2.86E+18	562	15.74	26.4	-10.7
Y – Axial	1.29E+19	562	48.63	47.2	1.5
V – Axial	2.27E+19	562	50.58	58.1	-7.5
<b>Average Bias: #4</b>					<b>-17.3</b>

Note:

- (1) Measured value was -14.9°F, but was set to 0°F per 2.2.1 step #1.

**Step #5**

Using a hypothetical end-of-life fluence of  $2.20 \times 10^{19}$  n/cm<sup>2</sup>, end-of-life irradiation temperature of 562°F, and measured initial  $RT_{NDT}$  of -8°F, the surface ART for this RPV material is predicted as follows:

$$ART = RT_u + \Delta RT + 2\sqrt{\sigma_u^2 + \sigma_{\Delta}^2} \text{ per Equation 1}$$

$$\Delta RT = \text{slope adjustment} \cdot TTS + \text{bias} \text{ per Equation 2}$$

Since the Section 2.2 method is followed, the bias is the average bias calculated in Table 3-2 and the slope adjustment is 1.

$$\sigma_{\Delta} = \sqrt{\sigma_{heat}^2 + \sigma_{multiplant}^2}$$

In this case, since only data from the plant of interest is being utilized,  $\sigma_{multiplant} = 0^\circ\text{F}$ . As a result,  $\sigma_{\Delta} = \sigma_{heat} = 16.4^\circ\text{F}$  for forgings per Table 2-2.

$$\text{In summary, } ART = RT_u + TTS + \text{Bias} + 2\sqrt{\sigma_u^2 + \sigma_{\Delta}^2}$$

$$\text{Therefore, } ART (^{\circ}\text{F}) = -8 + 57.4 - 17.3 + 2 * \sqrt{0^2 + 16.4^2}$$

$$ART = 64.9^\circ\text{F}$$

Note that the value of 16.4°F from Table 2-2 can be used in the margin term, because the prediction fluence is less than the fluence of the highest fluence capsule. If the fluence were above the fluence of the highest fluence capsule (above  $2.27 \times 10^{19}$  n/cm<sup>2</sup> in this case) the calculated E900-15 standard deviation term (25.1°F in this case) must be used instead. Since this specific forging heat is only in one plant, the 11°F of multi-plant uncertainty determined in Section 4.3.5 need not be considered.

Figure 3-1 shows the measured TTS data compared to the unadjusted E900-15 prediction. E900-15 tends to over-predict the measured TTS for this forging. The average heat-specific bias is calculated in Table 3-2 as -17.3°F. Figure 3-2 shows the bias corrected (average residual) E900-15 prediction. Both Figure 3-1 and Table 3-2 use the Table 3-1 inputs and a temperature of 562°F. Notice that the  $2\cdot\sigma$  uncertainty bands are reduced to  $2\cdot\sigma_{heat}$  for forgings of 16.4°F in the fluence range containing the measured data and then increase to  $\sigma_{ETC}$  above the highest fluence TTS point. As can be seen in these Figures, the data is characterized much better by the adjusted E900-15 equation, and all of the data is still bounded by two standard deviations.

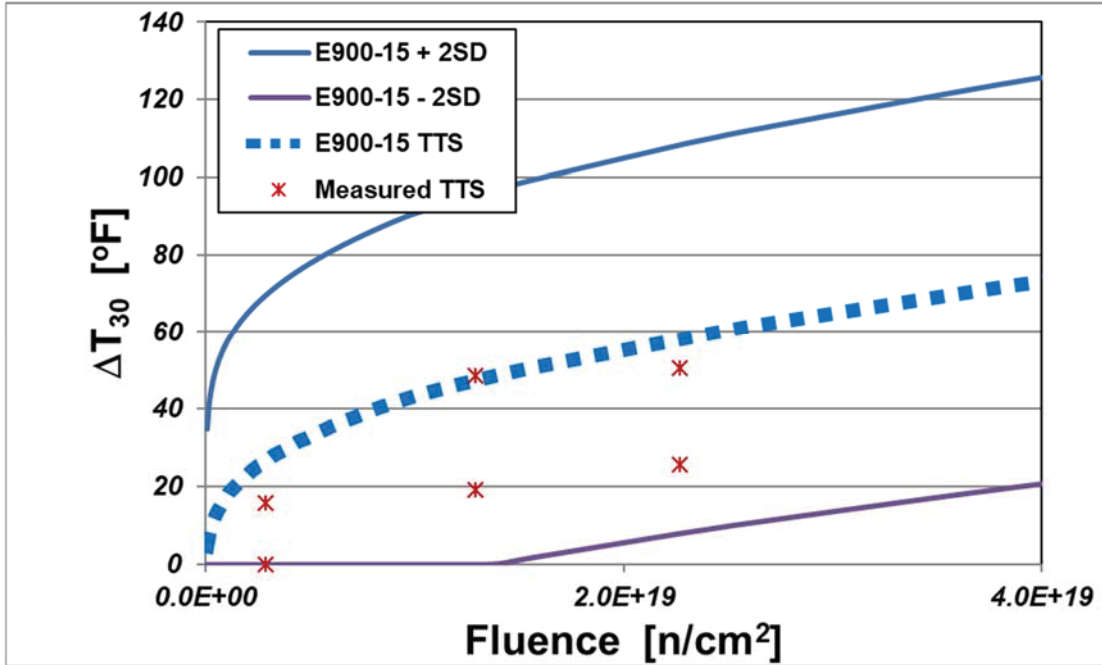


Figure 3-1 Intermediate Shell Forging E900-15 Prediction Compared to Measured TTS

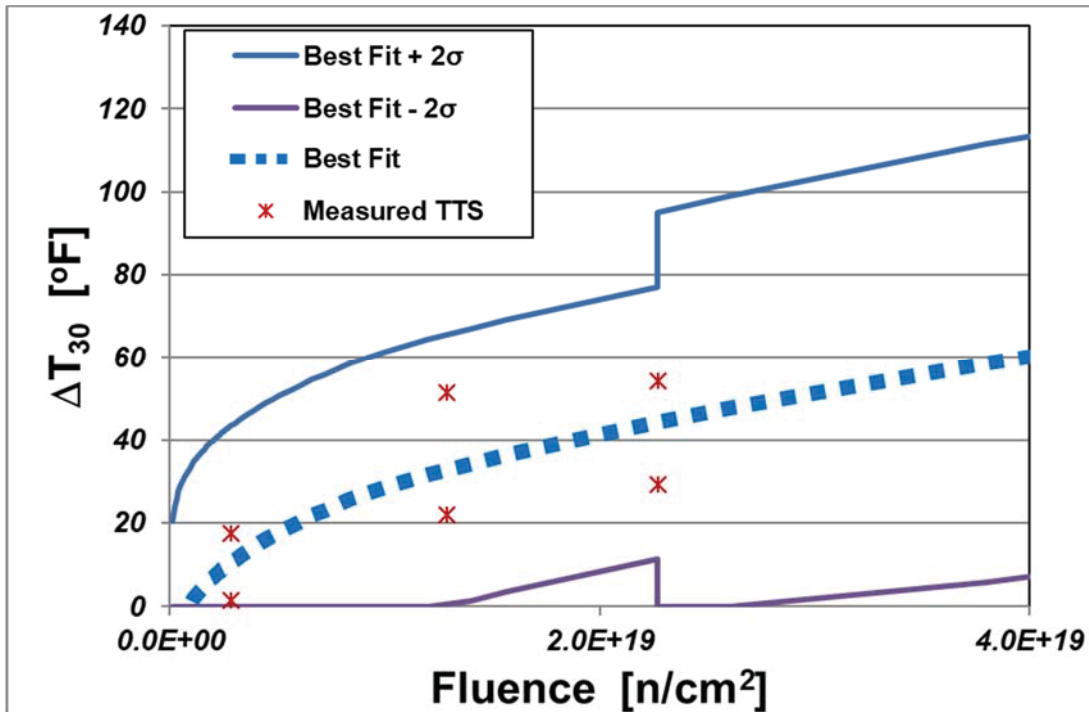


Figure 3-2 Intermediate Shell Forging E900-15 Adjusted Prediction Compared to Measured TTS #5

### 3.2 PLATE HEAT B6903

An example is presented for the PWR Plate Heat B6903, which was irradiated in five capsules. The data is taken primarily from [12]. Since the number of capsules is five or more, the Section 2.3 method is used. The best estimate chemistry for this plate is presented in Table 3-3. The measured and predicted TTS results are presented in Table 3-4. Step numbers from Section 2.3.1 are preceded by “#”.

<b>Table 3-3 Plate Heat B6903 Best Estimate Chemistry and Projected RPV Temperature (#1 and #3)<sup>(1)</sup></b>	
<b>Element</b>	<b>RPV Input</b>
Cu (wt %)	0.20
Ni (wt %)	0.54
P (wt %)	0.010
Mn (wt %)	1.31
Projected Average Temperature (°F)	542 (hypothetical)

Note:

- (1) In this case, the chemistry of the surveillance material and the RPV material are identical. Thus, the chemistry inputs are applicable to both steps #1 and #3 of the Section 2.3.1 method.

Table 3-4 Plate Heat B6903 TTS Data

Capsule	Fluence (E > 1 MeV)	Irradiation Temp. (°F) #1	Measured TTS (°F) #1	E900-15 Prediction for Measured TTS (°F) #2	E900-15 RPV Predicted TTS (°F) #4	TTS Adjust- ment (°F) #5	Adjusted Measured TTS (°F) #6	Best-Fit Prediction (°F) #7a	Residual (°F) #7b	Residual <sup>2</sup> (°F) #7c	
V – LT	3.02E+18	548 <sup>(1)</sup>	127.9	86.6	91.9	5.4	133.3	115.1	-18.1	328.4	
U – LT	6.20E+18	543	118.3	112.1	113.2	1.1	119.4	134.0	14.6	213.4	
W – LT	9.54E+18	543	147.7	126.6	127.9	1.3	149.0	147.1	-1.9	3.6	
Y – LT	2.10E+19	543	141.7	145.1	146.6	1.5	143.2	163.6	20.4	418.1	
X – LT	5.07E+19	543	175.8	177.6	179.4	1.8	177.6	192.7	15.1	229.2	
V – TL	3.02E+18	548 <sup>(1)</sup>	138.0	86.6	91.9	5.4	143.4	115.1	-28.2	796.4	
U – TL	6.20E+18	543	132.1	112.1	113.2	1.1	133.2	134.0	0.8	0.7	
W – TL	9.54E+18	543	180.2	126.6	127.9	1.3	181.5	147.1	-34.4	1183.4	
Y – TL	2.10E+19	543	166.9	145.1	146.6	1.5	168.4	163.6	-4.8	22.6	
X – TL	5.07E+19	543	179.0	177.6	179.4	1.8	180.8	192.7	11.9	142.5	
							Slope adjustment: 0.887; bias: 33.6 <sup>(2)</sup>		Sum <sup>(3)</sup> #7d:	3338.2	

Notes:

1. Actual irradiation temperature was 543°F; however, 548°F is used to demonstrate that each predicted TTS can have different inputs.
2. Bias limited by Table 2-4.
3. Minimized per #7e.

**Step #8**

Using a hypothetical end-of-life fluence of  $5.89 \times 10^{19}$  n/cm<sup>2</sup>, end-of-life irradiation temperature of 542°F, and measured initial RT<sub>NDT</sub> of 13.1°F, the surface ART for this RPV material is predicted as follows:

$$ART = RT_u + \Delta RT + 2\sqrt{\sigma_u^2 + \sigma_{\Delta}^2} \text{ per Equation 1}$$

$$\Delta RT = TTS + (\text{slope adjustment} - 1) \cdot TTS_{\text{highestfluence}} + \text{bias} \text{ per Equation 4}$$

Since the Section 2.3 method is followed, the bias and slope adjustment values calculated in Table 3-4 are utilized. In this case, Equation 4 is used in lieu of Equation 2, because the prediction is above the maximum capsule fluence, and the calculated best-fit slope (0.887) is less than 1.

In summary,

$$ART = RT_u + TTS + (\text{slope adjustment} - 1) \cdot TTS_{\text{highestfluence}} + \text{bias} + 2\sqrt{\sigma_u^2 + \sigma_{\Delta}^2}$$

$$ART (\text{°F}) = 13.1 + 186.8 + (0.887-1) \cdot 179.4 + 33.6 + 2 \cdot \sqrt{0^2 + 25.3^2}$$

$$ART = 263.8\text{°F}$$

Note that the value of 25.3°F is the calculated standard deviation from E900-15 (SD<sub>ETC</sub>). This value is used, because the fluence at which the prediction is being made ( $5.89 \times 10^{19}$  n/cm<sup>2</sup>) is greater than the fluence of the highest fluence capsule ( $5.07 \times 10^{19}$  n/cm<sup>2</sup>). The value of 13.3°F from Table 2-2 could be used in the margin term if the fluence for the prediction were below the fluence of the highest fluence capsule (below  $5.07 \times 10^{19}$  n/cm<sup>2</sup> in this case). Since Plate Heat B6903 is only in the plant being evaluated, the 11°F of multi-plant uncertainty determined in Section 4.3.5 need not be considered. Also, the multi-plant uncertainty is not added when SD<sub>ETC</sub> is used.

Figure 3-3 shows the measured TTS data compared to the E900-15 prediction. E900-15 tends to under-predict the measured TTS for this plate. The heat-specific slope and bias adjustment are calculated in Table 3-4 by minimizing the sum of the squared residual errors. Figure 3-4 shows the adjusted corrected (best-fit) E900-15 prediction. Both Figure 3-3 and Figure 3-4 use the Table 3-3 inputs and a temperature of 542°F for the ETC equations. For Figure 3-3 and Figure 3-4, the measured data is adjusted to the best-estimate input values (chemistry and temperature) to show a direct comparison on one plot. The  $2\sigma$  uncertainty bands are reduced to  $\sigma_{\text{heat}}$  for plates of 13.3°F in the fluence range containing the measured data and then increased to  $\sigma_{\text{ETC}}$  above the highest fluence TTS point. As can be seen in these figures, the data is characterized better by the adjusted E900-15 equation, and the data is appropriately bounded by the prescribed margin.



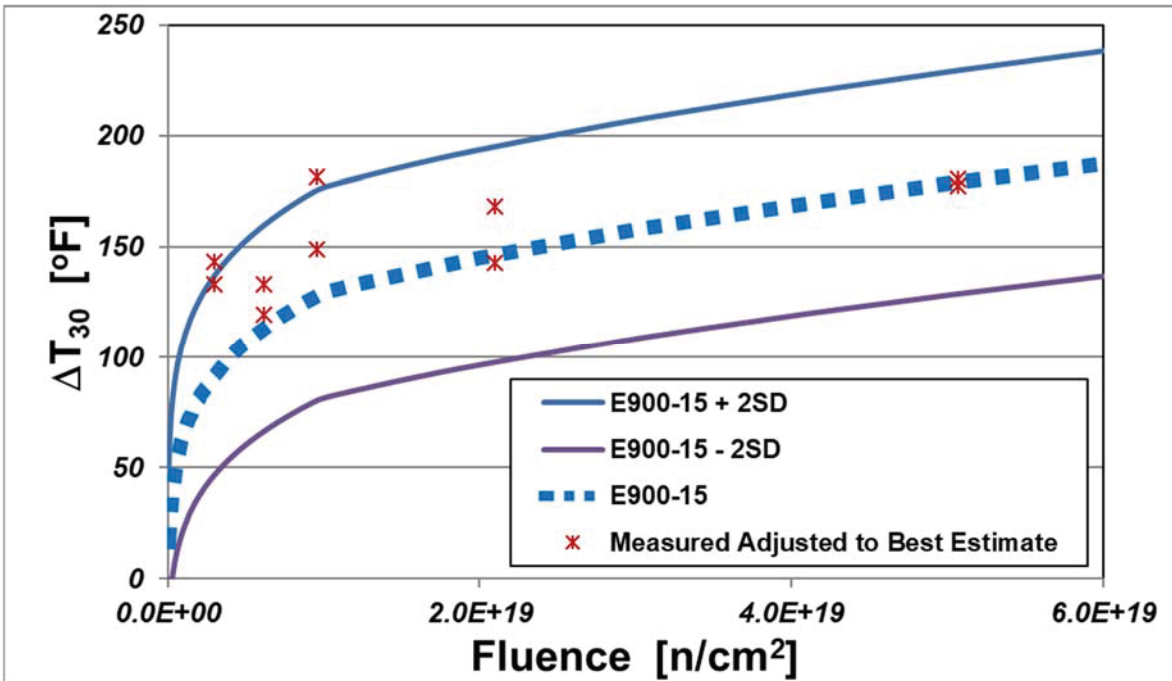


Figure 3-3 Plate Heat B6903 E900-15 Prediction Compared to Measured TTS

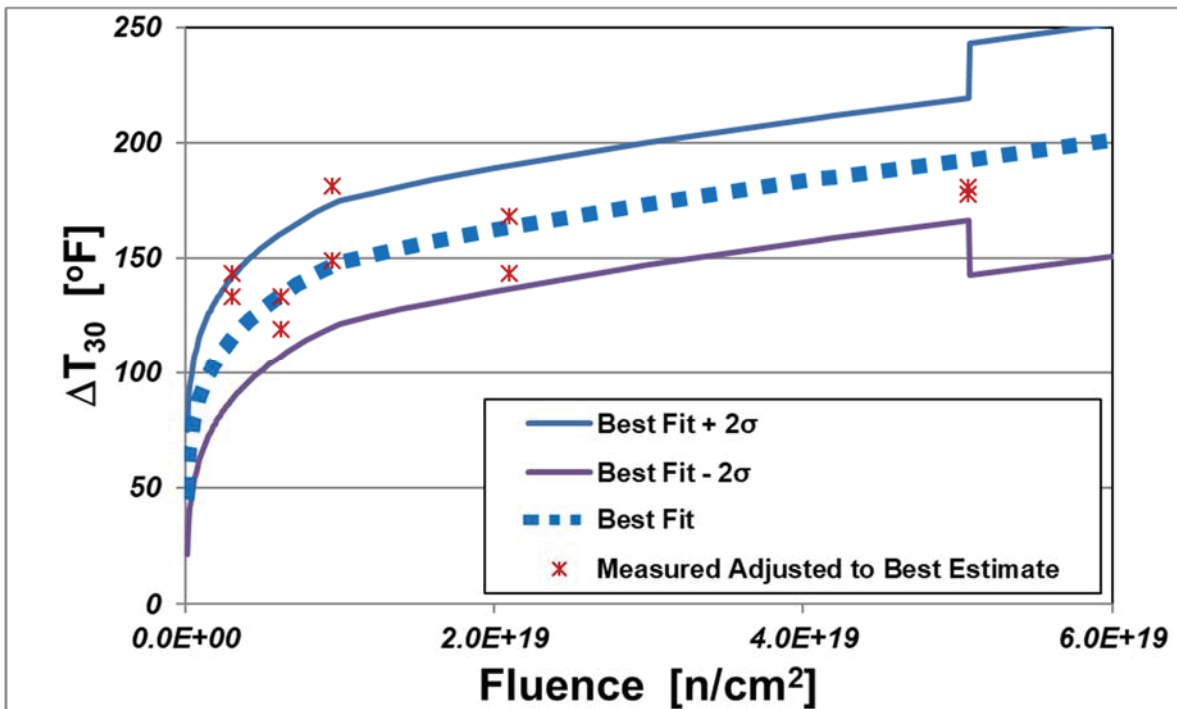


Figure 3-4 Plate Heat B6903 E900-15 Adjusted Prediction Compared to Measured TTS

### 3.3 WELD HEAT 895075

An example is presented for the Weld Heat 895075 which was irradiated in twelve capsules in four different plants. The data came primarily from [13] with some material-specific chemistries coming from plant-specific surveillance capsule reports. Since the number of capsules is five or more, the Section 2.3 method is used. The best-estimate chemistry for a hypothetical RPV material is presented in Table 3-5. For this example, the hypothetical material properties were taken to be the average of the capsule values in Table 3-6; however, for specific applications, the true best-estimate properties for the RPV material of interest should be used. The surveillance material chemistry as well as the measured and predicted TTS results are presented in Table 3-6. Step numbers from Section 2.3.1 are preceded by “#”.

<b>Element</b>	<b>RPV Input</b>
Cu (wt %)	0.039
Ni (wt %)	0.74
P (wt %)	0.014
Mn (wt %)	1.84
Projected Average Temperature (°F)	559.4

Table 3-6 Weld Heat 895075 TTS Data

Capsule #1	Cu (wt. %) #1	Ni (wt. %) #1	P (wt. %) #1	Mn (wt. %) #1	Fluence (x 10 <sup>19</sup> E > 1 MeV) #1	Irrad. Temp. (°F) #1	Measured TTS (°F) #1	E900-15 Prediction for Measured TTS (°F) #2	E900-15 RPV Predicted TTS (°F) #4	Adjusted Measured TTS (°F) #6	Best-Fit Prediction (°F) #7a	Resid. (°F) #7b	Residual <sup>2</sup> (°F) #7c
WB2-U	0.033	0.70	0.0125	1.885	0.604	559	32.6	21.1	21.5	33.1	20.4	-12.7	161.1
Cat1-Z	0.05	0.73	0.015	1.73	0.286	562	1.9	13.6	14.1	2.4	17.9	15.5	240.4
Cat1-Y	0.05	0.73	0.015	1.73	1.29	562	17.8	32.1	33.2	18.9	24.3	5.4	29.2
Cat1-V	0.05	0.73	0.015	1.73	2.27	562	26.5	44.3	45.7	28.0	28.5	0.5	0.3
WB1-U	0.03	0.75	0.0125	1.955	0.447	560	0.0 <sup>(1)</sup>	18.0	18.1	0.1	19.2	19.1	365.0
WB1-W	0.03	0.75	0.0125	1.955	1.08	560	30.5	29.8	30.0	30.7	23.2	-7.5	56.5
WB1-X	0.03	0.75	0.0125	1.955	1.71	560	25.8	38.7	38.9	26.1	26.2	0.1	0.0
WB1-Z	0.03	0.75	0.0125	1.955	2.40	560	13.9	46.9	47.2	14.2	29.0	14.7	217.4
MG2-V	0.04	0.74	0.016	1.81	0.302	557	38.5	15.2	14.5	37.8	18.0	-19.8	392.7
MG2-X	0.04	0.74	0.016	1.81	1.38	557	35.9	36.1	34.5	34.3	24.7	-9.6	92.6
MG2-U	0.04	0.74	0.016	1.81	1.90	557	23.8	43.3	41.3	21.9	27.0	5.1	26.2
MG2-W	0.04	0.74	0.016	1.81	2.82	557	43.8	54.2	51.8	41.3	30.5	-10.9	117.8
Slope adjustment: 0.335; bias: 13.2										Sum <sup>(2)</sup> #7d:			1699.1

Notes:

(1) The measured value is -6.4°F; however it is set to 0°F per step #1 of the Section 2.3.1 method.

(2) Minimized per step #7e

**Step #8, Example 1**

Using a hypothetical end-of-life fluence of  $2.70 \times 10^{19}$  n/cm<sup>2</sup>, end-of-life irradiation temperature of 559.4°F, and measured initial RT<sub>NDT</sub> of -50°F, the surface ART for this RPV material is predicted as follows:

$$ART = RT_u + \Delta RT + 2\sqrt{\sigma_u^2 + \sigma_{\Delta}^2} \text{ per Equation 1}$$

$$\Delta RT = \text{slope adjustment} \cdot TTS + \text{bias} \text{ per Equation 2}$$

Since the Section 2.3 method is followed, the slope adjustment and bias are the best-fit values from Table 3-6.

$$\sigma_{\Delta} = \sqrt{\sigma_{\text{heat}}^2 + \sigma_{\text{multiplant}}^2}$$

In this case, since data from more than just the plant of interest is being utilized,  $\sigma_{\text{multiplant}} = 11^{\circ}\text{F}$ .  $\sigma_{\text{heat}} = 16.9^{\circ}\text{F}$  for welds per Table 2-2.

$$\text{In summary, } ART = RT_u + \text{slope adjustment} \cdot TTS + \text{Bias} + 2\sqrt{\sigma_u^2 + \sigma_{\text{heat}}^2 + \sigma_{\text{multiplant}}^2}$$

$$ART (^{\circ}\text{F}) = -50 + 0.335 \cdot 50.5 + 13.2 + 2 \cdot \sqrt{0^2 + 16.9^2 + 11^2}$$

$$ART = 20.4^{\circ}\text{F}$$

Note that the value of 16.9°F from Table 3-2 can be used in the margin term, because the prediction fluence is less than the fluence of the highest fluence capsule. Additionally, because not all of the capsule data corresponds to the plant of interest, the additional 11°F of uncertainty developed in Section 4.3.5 is included in the margin term. If the fluence were above the fluence of the highest fluence capsule (above  $2.82 \times 10^{19}$  n/cm<sup>2</sup> in this case) the calculated E900-15 standard deviation term (25.3°F in this case) must be used instead.

**Step #8, Example 2**

Using a hypothetical end-of-life fluence of  $4.0 \times 10^{19}$  n/cm<sup>2</sup>, end-of-life irradiation temperature of 559.4°F, and measured initial  $RT_{NDT}$  of -50°F, the surface ART for this RPV material is predicted slightly differently than in the previous example. In this case, since the fluence of interest ( $4.0 \times 10^{19}$  n/cm<sup>2</sup>) is higher than the highest fluence capsule (above  $2.82 \times 10^{19}$  n/cm<sup>2</sup>), and Equation 4 must be utilized.

$$ART = RT_u + \Delta RT + 2\sqrt{\sigma_u^2 + \sigma_{\Delta}^2} \text{ per Equation 1}$$

$$\Delta RT = TTS + (\text{slope adjustment} - 1) \cdot TTS_{\text{highest fluence}} + \text{bias} \text{ per Equation 4}$$

Since the Section 2.3 method is followed, the best-fit bias and slope adjustment values calculated in Table 3-6 are utilized. In this case, Equation 4 is used in lieu of Equation 2, because the prediction is above the maximum capsule fluence, and the calculated best-fit slope (0.335) is less than 1.

In summary,

$$ART = RT_u + TTS + (\text{slope adjustment} - 1) \cdot TTS_{\text{highest fluence}} + \text{bias} + 2\sqrt{\sigma_u^2 + \sigma_{\Delta}^2}$$

$$ART (\text{°F}) = -50 + 63.2 + (0.335-1) \cdot 51.8 + 13.2 + 2 \cdot \sqrt{0^2 + 26.3^2}$$

$$ART = 44.5^{\circ}\text{F}$$

Note that the value of 16.9°F from Table 3-2 cannot be used in the margin term, because the prediction fluence is greater than the fluence of the highest fluence capsule. Thus, the calculated E900-15 standard deviation term ( $SD_{ETC}$ , 26.3°F in this case) must be used instead. Additionally, when  $SD_{ETC}$  is used for  $\sigma_{\Delta}$ , the additional 11°F of uncertainty developed in Section 4.5 need not be included in the margin term.

Figure 3-5 shows the measured TTS data compared to the E900-15 prediction. In this case, while the E900-15 bias is not large, there is very little embrittlement increase with fluence. In other words, the slope does not agree with E900-15 prediction. The heat-specific bias is calculated in Table 3-6. Figure 3-6 shows the adjusted (best-fit) E900-15 prediction. Both Figure 3-5 and Figure 3-6 use the Table 3-6 inputs and a temperature of 559.4°F for the ETC equations. For Figure 3-5 and Figure 3-6, the measured data is adjusted to the hypothetical RPV chemistry input values (chemistry and temperature) to show a direct comparison on one plot. The  $2 \cdot \sigma$  uncertainty bands are reduced to  $2 \cdot \sigma_{\text{heat}}$  of 16.9°F for welds combined with the  $\sigma_{\text{multiplant}}$  of 11°F since the data was irradiated in multiple plants inside the fluence range. These uncertainties are combined with the square root of the sum of the squares to yield  $\sigma = 20.2^{\circ}\text{F}$ . The value of 20.2°F is used in the fluence range containing the measured data and then increased to  $\sigma_{ETC}$  above the highest fluence TTS point. Note that the slope is reduced within the fluence range of the measured data, but then the slope is adjusted back to be identical to the E900 slope once the highest measured fluence

point is reached per Equation 4. Thus, the Figure 3-5 prediction line is parallel to the Figure 3-6 prediction line above the highest measured fluence point. As can be seen in Figure 3-5 and Figure 3-6, the data is better characterized by the adjusted E900-15 equation, and the data is all bounded by two standard deviations.

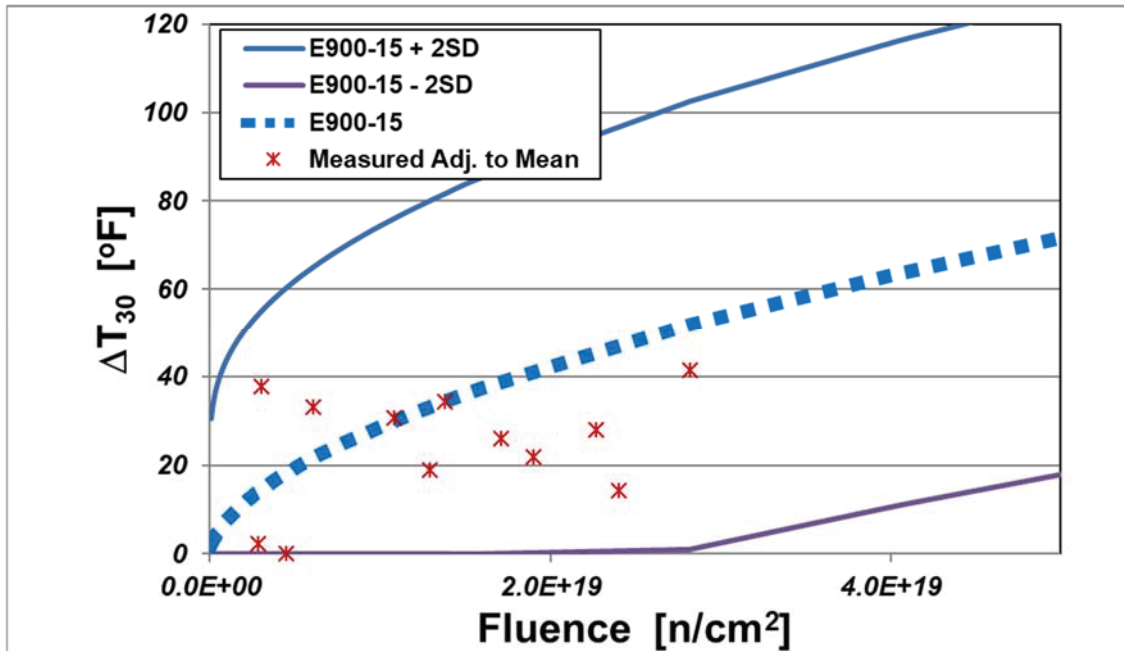


Figure 3-5 Weld Heat 895075 E900-15 Prediction Compared to Measured TTS

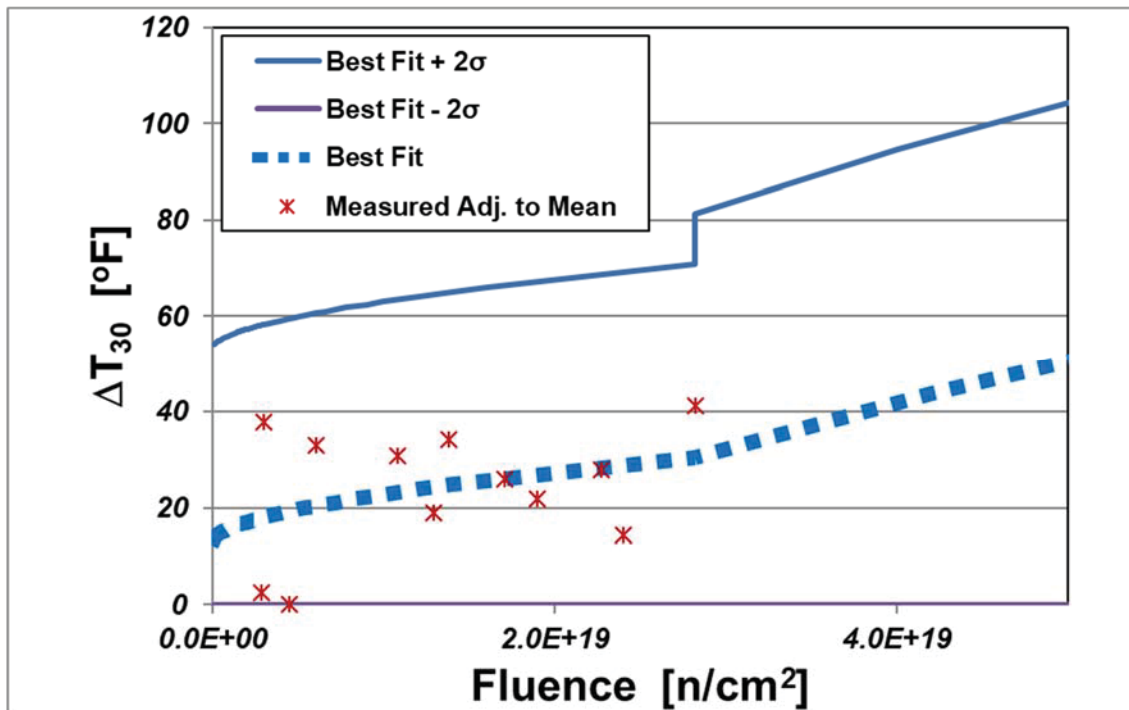


Figure 3-6 Weld Heat 895075 E900-15 Adjusted Prediction Compared to Measured TTS

## 4 METHOD DEVELOPMENT

After consideration of the methods described in Appendix A, the following approach was developed. The approach taken herein is deterministic and accounts for the mean heat-specific trend and associated uncertainty.

ASTM Standard Guide E900-15 [5] is the most recent internationally accepted consensus standard for predicting RPV embrittlement. ASTM Subcommittee E10.02 undertook a five-year effort, culminating in 2015 with a major revision to ASTM E900 as documented in [8]. The E900-15 ETC is based on a fit to measured power reactor transition temperature shift (TTS; 30 ft-lb Charpy V-Notch) data from surveillance programs conducted in 13 different nations comprising the most comprehensive collection of evidence concerning neutron irradiation embrittlement in non-VVER RPV-grade steels available. Additionally, the NRC has stated its intention to adopt the E900-15 ETC should it decide to develop a Revision 3 to Regulatory Guide 1.99 [6]. For these reasons, the proposed embrittlement Code Case is intended to be written with ETC acceptability criteria which E900-15 meets. Therefore, use of E900-15 and its underlying database are used in developing the methodology presented herein. However, the general methods described herein considering heat-specific measurement data could be utilized with a different ETC. The uncertainty terms developed herein are specific to E900-15 and the associated database.

### 4.1 EMBRITTLEMENT SHIFT

For the reasons mentioned above, the TTS ETC defined in E900-15 is used with heat-specific adjustments based on measured surveillance data. The approach taken in both the U.S. (RG1.99R2) and in Japan (JEAC4201) when considering heat-specific data is to adjust the respective ETC to fit the measured plant specific data [1]. The U.S. and Japanese approaches are different in that the RG1.99R2 [3] applies a best-fit chemistry factor essentially resulting in a multiplicative factor replacing the generic chemistry factors when the data is deemed “credible.” Whereas the Japanese approach applies an additive offset to force the ETC through the mean of the measured TTS values. JEAC4201 requires two or more measurements for the  $\sigma$  to be reduced from 22°C (40°F) to 18°C (32°F). RG1.99R2 also requires two or more data points and the data to be “credible” (scatter less than or equal to the ETC scatter) for the embrittlement  $\sigma$  to be reduced by half. The basis for reduction by half is unknown.

With consideration of the current U.S. and Japanese approaches, the approach described in Section 2 is proposed depending on the number of capsules tested containing the material of interest and the projected fluence.

With measurement from one capsule (one irradiation condition), the amount of heat-specific data was judged to be insufficient to adjust the ETC TTS prediction. There is significant uncertainty in individual measured TTS values and the database used to develop E900-15 ETC is extensive and therefore considered to be reasonably accurate in representing the heat-specific data.

With the measurement of two or more irradiation conditions for a single heat, there is sufficient information to determine the average bias of the ETC prediction relative to the heat-specific measured TTS values. The knowledge of the heat-specific measurements provides more



certainty and the inability of the ETC to predict differences between heats can be eliminated. The adjustment of the ETC based on two or more capsules is consistent with RG1.99R2.

The knowledge of five or more heat-specific measurements provides more certainty such that the fluence trend deviation from the ETC can be corrected. A minimum of five independent fluence TTS values was selected using engineering judgement. Through analysis of several sample data sets, five or more TTS values produced fluence trends that were reasonable; however, with fewer data sets fluence adjustments were not reasonable at times. The slope adjustment was deemed of value since some datasets showed significant deviations from the E900-15 fluence trend which could be corrected. Adjusting for a fluence trend different from the ETC reduces the heat-specific residual standard deviation. However, since the datasets are still relatively small for calculation of standard deviation, the  $\sigma_{\text{heat}}$  is conservatively used within the measured fluence range. To protect for potential non-conservative trend corrections when predicting at fluences greater than the measured TTS fluence values, the slope adjustment is restricted to be one or more.

## 4.2 UNCERTAINTY DETERMINATION

E900-15 does not predict TTS perfectly for any heat of material. Thus, when comparing the prediction to the measured TTS value there is a residual (TTS prediction – TTS measured). For a given heat, the average of the residuals determines the average bias (average error). The  $\sigma$  (standard deviation) of all the average heat biases for each product form is referred to herein as  $\sigma_{\text{bias}}$ .  $\sigma_{\text{bias}}$  represents model uncertainty as a result of the ETC being derived from many different heats for which the ETC does not adequately address, hence heat-specific biases. The biases are also due to irradiation in different plants and possibly other factors. If only one heat (irradiated in one plant) was considered in the development of the ETC, the  $\sigma_{\text{bias}}$  would be zero, because the average error would be zero for that heat since it is the only heat considered.

The  $\sigma$  of the residuals of a specific heat's data points between the ETC prediction and the measured TTS values is the  $\sigma_{\text{heat}}$ .  $\sigma_{\text{heat}}$  represents the uncertainty if the ETC were based solely on one heat irradiated in one plant and would include uncertainties on measurement, material variability, some model uncertainty, etc.

Assuming that  $\sigma_{\text{bias}}$  and  $\sigma_{\text{heat}}$  are the only components of  $SD_{\text{ETC}}$ , combining these uncertainties in quadrature should yield the E900-15 average  $SD_{\text{ETC}}$  as shown in Equation 5. Each term developed in the following sections is checked for reasonable agreement with Equation 5.

**Equation 5** 
$$SD_{\text{ETC}} \cong \sqrt{\sigma_{\text{bias}}^2 + \sigma_{\text{heat}}^2}$$

In most cases, a reliable  $\sigma_{\text{heat}}$  cannot be determined for a given heat because the sample size is too small for a single surveillance program heat. Surveillance shift measurements irradiated in a single plant typically do not exceed 12 (and most are much less). However, the standard deviation of all the residuals for a product form used in the E900-15 database can be used to calculate a generic  $\sigma_{\text{heat}}$  for each product form. This assumes that each heat has similar  $\sigma$  which is the case since the steels in the database are all nuclear RPV steel manufactured to similar specifications. As described in Section 4.3 various factors are evaluated to check for correlations with  $\sigma$ . Lacking

any  $\sigma$  correlations with various heat differences,  $\sigma_{\text{heat}}$  can be considered representative of all the heats within the product form.

The E900-15  $SD_{\text{ETC}}$  is dependent on product form and predicted TTS. To determine the  $\sigma_{\text{heat}}$  for each product form, the E900-15 PLOTTER database [8] was used. The data was filtered for data with heat IDs and at least three measurements from each heat. The TTS was predicted for each data point using the E900-15 TTS equation and the residual was determined (TTS prediction – TTS measured). The  $\sigma$  and mean bias for each heat were determined. Each heat's residuals were corrected for the heat mean bias and the  $\sigma_{\text{heat}}$  was calculated for each product form as the standard deviation of the average heat bias adjusted residuals. These values were developed using the E900 ETC as described in Section 2 and summarized in Table 2-2. Note that as described in Section 2, the Table 2-2 values are only recommended for use when capsule data exists at a fluence greater than or equal to the fluence of interest and when multiple tested capsules exist.

### 4.3 DERIVATION OF UNCERTAINTY TERMS

The international TTS database used for development of ASTM E900-15 and available from ASTM [8] was used to derive uncertainty terms when using surveillance data. Specifically, the BASELINE data subset was used, which is the same dataset used to assess and calibrate the E900 ETC. Reference [8] describes the BASELINE data subset as follows:

*To be in the BASELINE subset the steel had to be of commercial grade, have all descriptive variables (copper, nickel, manganese, phosphorus, fluence, flux, temperature, and product form) known, been exposed to neutron irradiation in a power reactor (PWR or BWR), and had embrittlement quantified by  $\Delta T_{41J}$  measured using full-size Charpy V-notch specimens. The BASELINE subset included 1,878  $\Delta T_{41J}$  surveillance data from 13 countries.*

The large surveillance database consisting of radiation-induced TTS and related information compiled by Subcommittee E10.02 [8] is accurate enough in total to develop uncertainty terms. According to [8]:

*Every effort was made to ensure the accuracy of the data used in this evaluation and its fidelity with respect to the source documents. To ensure accuracy, data from the largest national data collections (USA, Japan, France, Germany, and Belgium) were double checked by national experts. Additionally, data from Brazil, Italy, Mexico, South Korea, Sweden, Switzerland, and Taiwan were entered from their surveillance reports by one Subcommittee member and double checked by another.*

Since the publication of the report, there are known to be isolated errors in the database. However, it was considered accurate enough to develop the E900-15 ETC and accurate enough to develop the  $SD_{\text{ETC}}$  terms for the various product forms published in ASTM E900-15. Thus, it is also considered accurate enough for use in development of associated uncertainty terms herein. If errors were noticed during this effort (for example, duplicate data entries), the errors were corrected.

Only heats with three or more TTS measurements were included. The goal of the analysis is to develop the  $\sigma_{\text{heat}}$  without including plant and temperature differences within a heat. Thus, heats that were irradiated in multiple plants were analyzed separately in Section 4.3.5 to develop an uncertainty term which is added for plant-to-plant effect on uncertainty, but not included for development of  $\sigma_{\text{heat}}$ .  $\sigma_{\text{heat}}$  is developed for each product form in the following sections.

#### 4.3.1 Determination of Weld Uncertainty Terms

There are 87 welds from the E900 PLOTTER database with at least three shift measurements from a single plant resulting in a total of 339 shift measurements. Note that for this analysis, identical heats that were irradiated in multiple plants were treated as separate heats. The largest heat dataset from a single plant contains six measurements. The residual bias (average error for the heat) and  $\sigma$  was determined for each heat. The individual residuals were corrected for each heat bias, and the resulting  $\sigma$  of the bias corrected residuals was calculated to be 16.9°F. This value can be considered the  $\sigma_{\text{heat}}$  for weld materials.

The validity of this  $\sigma_{\text{heat}}$  value was checked by comparing it, combined with the  $\sigma_{\text{bias}}$ , to the E900-15  $SD_{\text{ETC}}$  for weld materials. The  $\sigma$  of the mean heat biases of the 87 heats is 23.7°F which represents  $\sigma_{\text{bias}}$  for weld materials. Combining  $\sigma_{\text{bias}}$  and  $\sigma_{\text{heat}}$  in quadrature per Equation 5 yields 29.1°F. The average E900-15 predicted shift for the 339 measurements is 105.1°F which yields a E900-15 predicted  $\sigma = 28.9^\circ\text{F}$  per Equation 3. These values are in excellent agreement as expected per Equation 5. A difference would be expected, because the 87 heats do not comprise the whole weld E900 database used to develop the E900-15  $SD_{\text{ETC}}$ .

Chemistry differences were investigated for effect on  $\sigma$ . No significant correlations were found with heat-specific  $\sigma$  values, therefore  $\sigma_{\text{heat}} = 16.9^\circ\text{F}$  is applicable to all welds. Figure 4-1 shows the bias adjusted weld data residuals versus fluence compared to  $2 \cdot \sigma_{\text{heat}}$ . The y-axis of Figure 4-1 represents the residual of a specific data point minus the average error (bias) for that heat. This adjustment was made to account for the fact that each heat has a specific “error” (mean bias vs. the ETC prediction). Thus, the y-axis represents a true within heat residual as adjusted for the heat’s average error. As seen in Figure 4-1,  $\pm 2 \cdot \sigma_{\text{heat}}$  appropriately bounds the majority of the data.

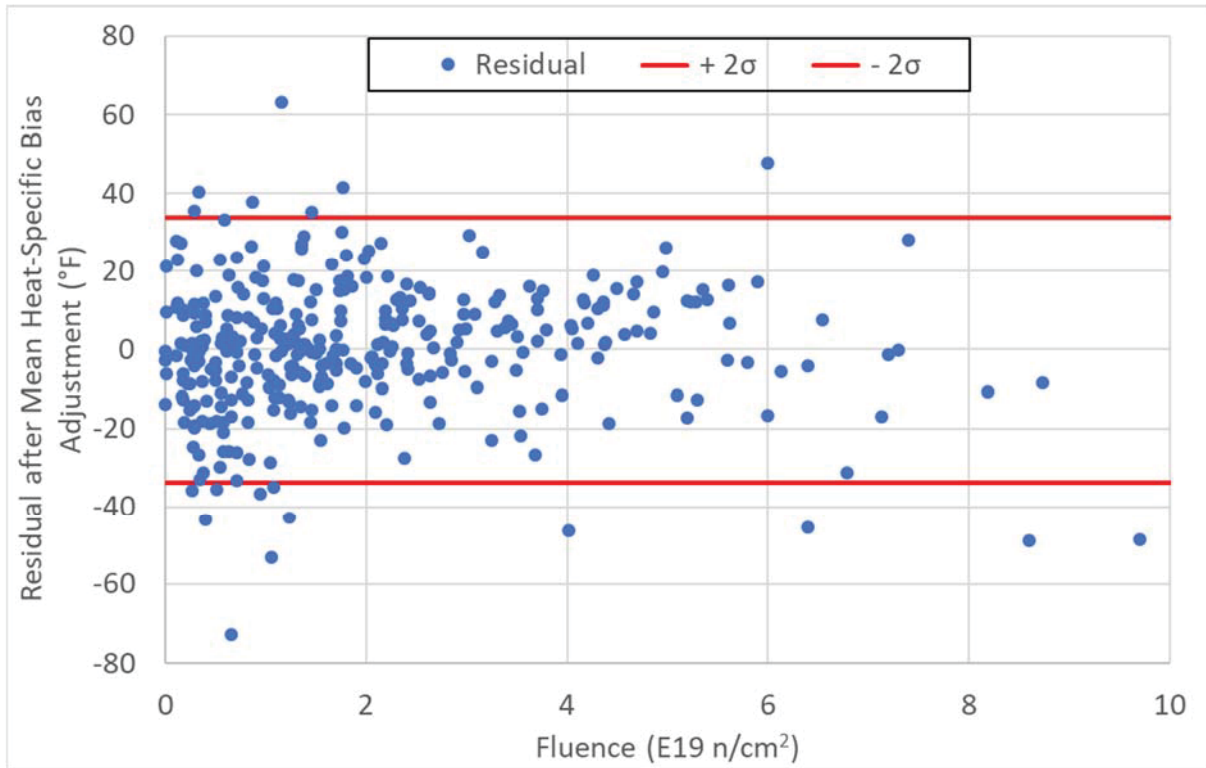


**Figure 4-1 Weld Error-Adjusted Residuals Compared to Twice  $\sigma_{\text{heat}}$  for Welds**

### 4.3.2 Determination of Forging Uncertainty Terms

There are 57 heats of forgings from the E900 PLOTTER database with at least three shift measurements for a total of 260 shift measurements. The largest heat dataset contains eight measurements. The residual bias (average error for the heat) and  $\sigma$  was determined for each heat. The individual residuals were corrected for each heat bias, and the resulting  $\sigma$  of the adjusted residuals was calculated to be 16.4°F. This value can be considered the  $\sigma_{\text{heat}}$  for forging materials.

The validity of this  $\sigma_{\text{heat}}$  value was checked by comparing it, combined with the  $\sigma_{\text{bias}}$ , to the E900-15  $SD_{\text{ETC}}$  for forging materials. The  $\sigma$  of the mean biases of the 57 heats is 18.9°F which represents  $\sigma_{\text{bias}}$  for forging materials. Combining these in quadrature per Equation 5 yields 25.0°F. The average E900-15 predicted shift is 62.7°F which yields a E900-15 predicted  $\sigma = 25.4^\circ\text{F}$  per Equation 3. These values are in very good agreement as expected per Equation 5. The values are expected to be slightly different because the 57 heats do not comprise the whole forging E900 database used to develop the E900-15  $SD_{\text{ETC}}$ .

Factors that might affect the heat-specific  $\sigma$  values were investigated including chemistry and forging country of origin (when identified): France, U.S., and Netherlands. The only factor causing significant differences in  $\sigma$  is Cu.  $\sigma$  was plotted against Cu and the  $R^2$  for the linear fit is 0.10

meaning there is not a strong correlation. There is one very high  $\sigma$  at 0.16% Cu. Removal of this potential outlier reduces  $R^2$  to 0.02, which is an insignificant correlation. There is one high fluence high shift point from Forging 7.1 in the PLOTTER database, which is an outlier relative to many ETCs as identified in Table 16 of the Adjunct [8]. This measured TTS was verified to be correct from the original reference [14]. This one point of 260 measurements does not justify a trend in  $\sigma$  with respect to Cu. Therefore,  $\sigma_{\text{heat}} = 16.4^\circ\text{F}$  for all forgings. Figure 4-2 shows the heat bias-adjusted forging data residuals versus fluence compared to  $2 \cdot \sigma_{\text{heat}}$ . As seen in Figure 4-2,  $\pm 2 \cdot \sigma_{\text{heat}}$  appropriately bounds the majority of the data.

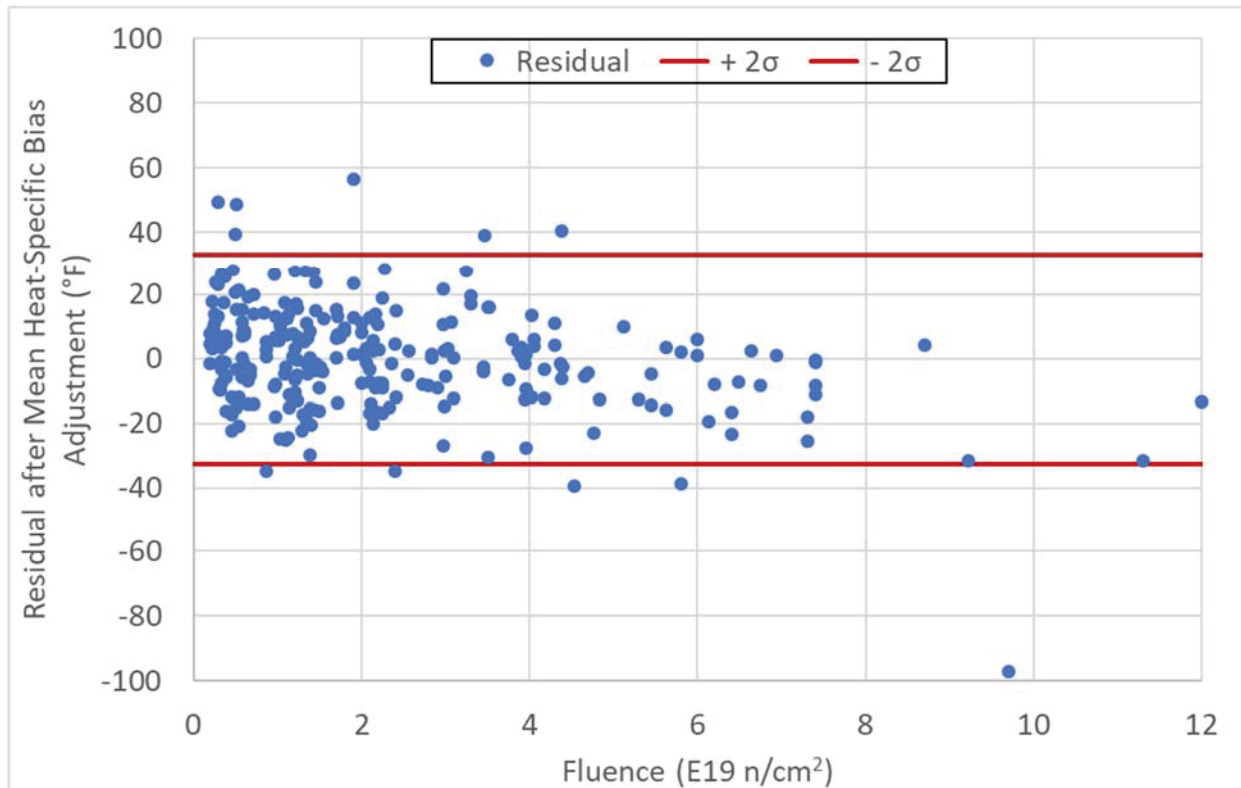


**Figure 4-2 Forging Error-Adjusted Residuals Compared to Twice  $\sigma_{\text{heat}}$  for Forgings**

### 4.3.3 Determination of Plate Uncertainty Terms

For plates there are 72 heats, excluding the standard reference materials (SRM), with at least three measurements and a heat ID for a total of 423 shift measurements. The data includes material from BWR and PWR designs in the U.S., Korea, and Taiwan with A-302B, A-302BM and A-533 specifications. SRM plate data was not included in this section since the SRM heats were irradiated in multiple plants and therefore different environments (e.g., different temperatures). The goal of this section is to identify the  $\sigma_{\text{heat}}$  not confounded by plant and temperature differences within a heat.

The residual bias (average error for the heat) and  $\sigma$  was determined for each heat. The individual residuals were corrected for each heat bias, and the resulting  $\sigma$  ( $\sigma_{\text{heat}}$ ) of the adjusted residuals was calculated to be 13.8°F. The  $\sigma$  of the mean heat-specific biases of the 72 heats is 16.8°F which is the  $\sigma_{\text{bias}}$ . Combining these in quadrature per Equation 5 yields 21.7°F. Average E900-15 predicted shift is 69.4°F which yields a E900-15 predicted  $\sigma = 21.5^\circ\text{F}$  per Equation 3. These values are in very good agreement as expected per Equation 5. The values are expected to be slightly different because the 72 heats do not comprise the whole plate E900 database used to develop the E900-15  $SD_{\text{ETC}}$ .

The plate heat  $\sigma$  values were checked for correlation with BWR vs. PWR and chemistry. Ni showed the only significant correlation. There are two groups for plates relative to Ni content with A-302B having low Ni and A-302BM and A-533B1 having higher Ni. Material groupings have been presented previously [15] with the specification differences being a reasonable delineation. Statistics for the material groupings are shown in Table 4-1. Using the method from Section 14.4 of NUREG-1475, Revision 1, [16] the F distribution 2-sided 95% confidence is 1.79. The variance ratio is variance of A-302B divided by high Ni variance =  $473/177 = 2.67$ . Since 2.67 is greater than 1.79, there is greater than 95% confidence level that the variances are different.

<b>Table 4-1 Plate Statistics</b>					
<b>Variable</b>	<b>#</b>	<b><math>\sigma</math></b>	<b>No. Heats</b>	<b>Variance</b>	<b>Degrees of Freedom</b>
A-302BM and A-533B bias adjusted residual	404	13.3	67	177	403
A-302B bias adjusted residual	19	21.8	5	473	18

The  $\sigma$  (21.8°F) for A-302B plates is approximately the same as the E900-15  $SD_{\text{ETC}}$  for plates, therefore use of surveillance data cannot be used to reduce  $\sigma_{\Delta}$  for A-302B plates. The heat  $\sigma$  values showed no significant correlation with Ni when only the high Ni plates (A-302BM and A-533B) were considered. Figure 4-3 shows the error adjusted high nickel plate data residuals versus fluence compared to  $2 \cdot \sigma_{\text{heat}}$ , where the  $\sigma_{\text{heat}}$  for high Ni plates is  $\sigma_{\text{heat}} = 13.3^\circ\text{F}$ . As seen in Figure 4-3,  $\pm 2 \cdot \sigma_{\text{heat}}$  appropriately bounds the majority of the data.

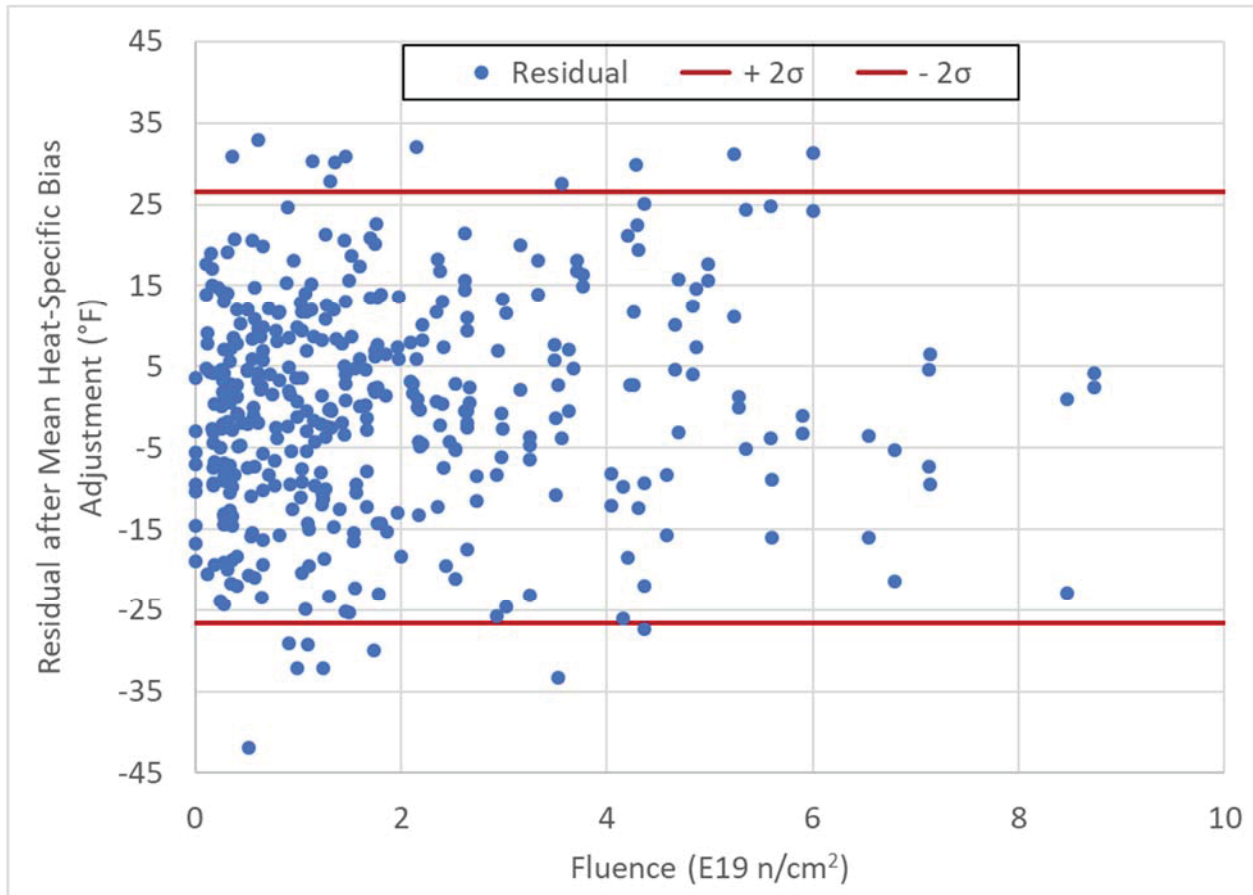


**Figure 4-3 Error-Adjusted Residuals Compared to Twice  $\sigma_{\text{heat}}$  for Higher Ni Plates**

#### 4.3.4 Standard Reference Material Plate Uncertainty Terms

The standard reference material (SRM) provides an ideal case to eliminate the small sample size factor issue in determining plate  $\sigma$  for evaluating heat-specific surveillance program sets. Three SRMs were irradiated in multiple surveillance programs. The average error (residual bias) and  $\sigma$  were determined for each heat. Each of the three heats have enough data to provide a meaningful  $\sigma$  and all resulted in a heat-specific  $\sigma$  value very similar to one another as shown in Table 4-2 with the average  $\sigma = 16.8^\circ\text{F}$ .

Heat	#	Mean of Residuals	$\sigma$
SASTM	26	3.9	16.6
SHSS01	18	-11.3	17.1
SHSS02	65	7.6	16.7

The SRM materials were irradiated at several temperatures and in different reactors. The average heat-specific  $\sigma = 16.8^{\circ}\text{F}$  captures the measurement uncertainty, model uncertainty on temperature effect prediction, and other differences in plant irradiation conditions. In addition, the full chemistry and material variability within each respective plate is included, since the ~200 to 800 Charpy specimens from each SRM plate would have been removed from various locations throughout the respective SRM plates. This variability explains why the  $\sigma = 16.8^{\circ}\text{F}$  for the SRM plates is larger than the  $\sigma_{\text{heat}} = 13.3^{\circ}\text{F}$  for the high nickel plates for which each heat was only irradiated in one reactor (see Section 4.3.3).

It is noted that the SASTM A-302B plate does not have a higher  $\sigma$  like the other A-302B plates in Section 4.3.3. Since there are only five A-302B plate heats in the database, the  $\sigma_{\text{heat}} = 21.8^{\circ}\text{F}$  from Section 4.3.3 has a high uncertainty and may not be representative. However, all five heats had high  $\sigma$  values.

Figure 4-4 shows  $\sigma$  calculated for each plate heat plotted against the sample size. As can be seen in the figure, scatter (variability) in  $\sigma$  is reduced with increasing sample size. The uncertainty of  $\sigma$  with sample sizes even up to 10 is large and, therefore, it is difficult to accurately determine  $\sigma$  from such a small sample size. Therefore, the  $\sigma$  of typical surveillance program data sets ( $\leq \sim 12$ ) should not be used as a criterion for screening data “credibility.”

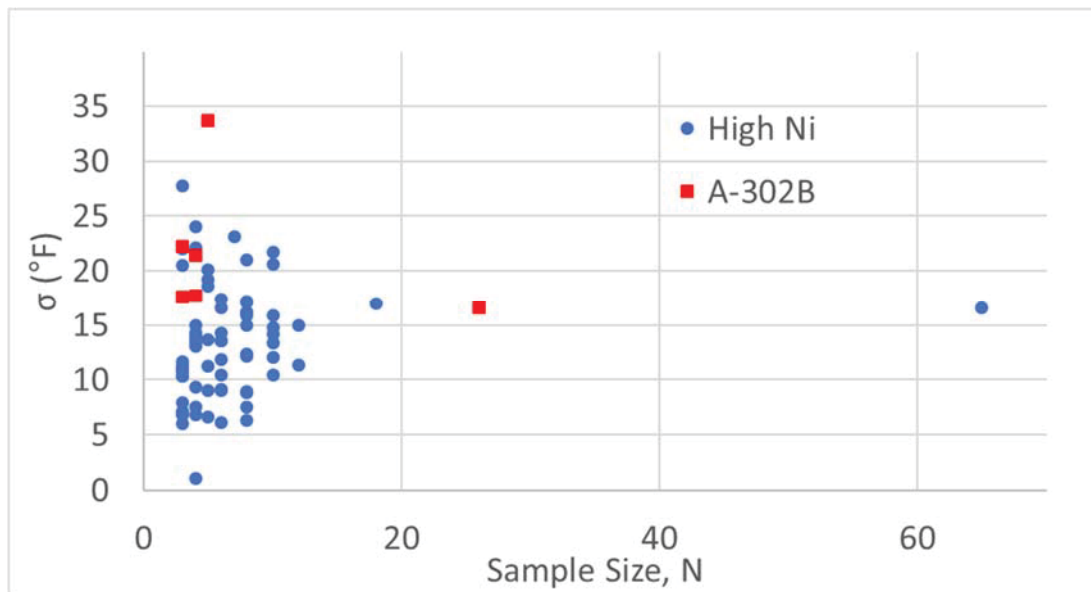


**Figure 4-4 Plate Heat-specific  $\sigma$  versus Sample Size**

( $N > 12$  are SRM plate heats which include increased uncertainty due to irradiation in multiple plants)



### 4.3.5 Uncertainty Determination for Multiple RPVs

The SRM heats were irradiated in multiple RPVs. To isolate the effect of plant differences, the average error (residual bias) and  $\sigma$  were determined for each plant with at least three SRM TTS measurements. Twenty plants had at least three measurements of one of the SRM heats totaling 72 TTS measurements. The data included the SASTMA A-302B heat and the SHSS02 A-533 SRM. The SHSS01 SRM did not contain any datasets of at least three from a single plant. The residuals were corrected for each plant bias and  $\sigma$  of the corrected residuals was calculated to be 11.9°F. This value can be considered the  $\sigma_{\text{heat}}$  for the SRM heats.

Figure 4-5 shows the plant bias-adjusted SRM plate data residuals versus fluence compared to  $2 \cdot \sigma_{\text{heat}}$ , where the SRM is  $\sigma_{\text{heat}} = 11.9^\circ\text{F}$ . One of the goals of this effort is to identify the  $\sigma_{\text{heat}}$  with and without consideration of plant differences and the inability for the ETC to adjust for temperature differences between plants. The resulting difference in uncertainty when using SRM  $\sigma_{\text{heat}}$  with and without plant differences can be calculated as shown in Equation 6.

**Equation 6** 
$$SRM \sigma_{\text{multiplant}} = \sqrt{16.8^\circ\text{F}^2 - 11.9^\circ\text{F}^2} = 11.9^\circ\text{F}$$

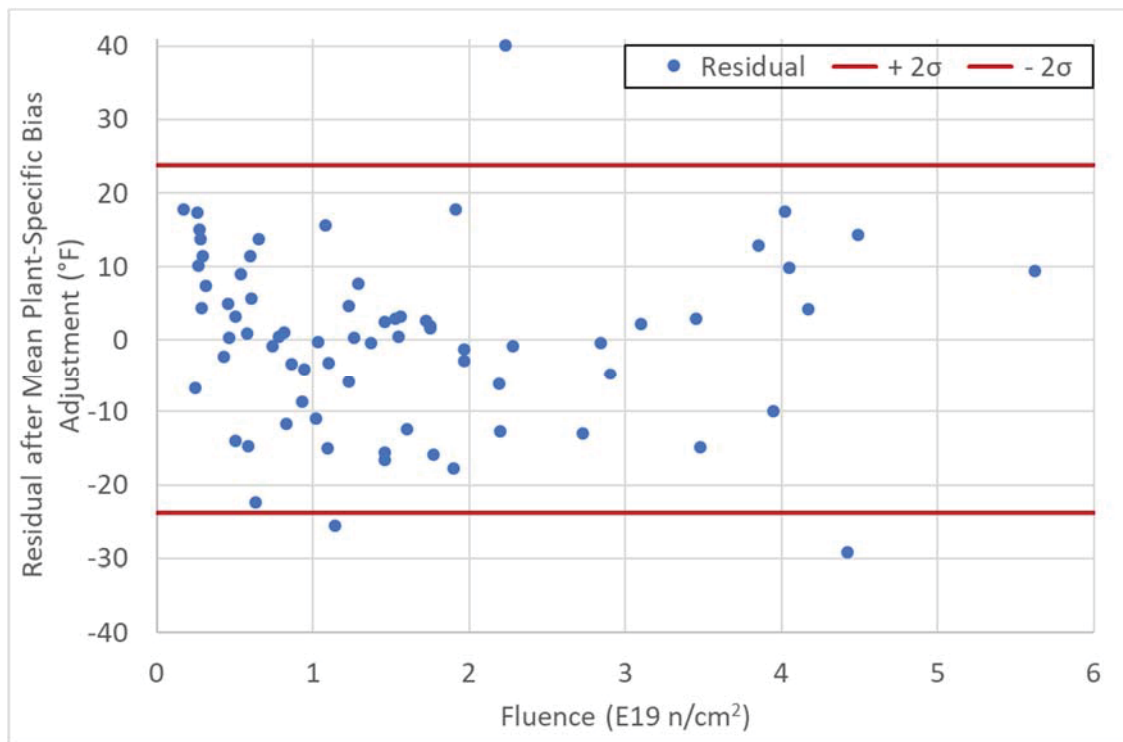


**Figure 4-5 Error-Adjusted Residuals Compared to Twice  $\sigma_{\text{heat}}$  for SRM Plates**

Some surveillance program weld heats were also irradiated in multiple plants. The  $\sigma_{\text{heat}} = 16.9^\circ\text{F}$  was already determined in Section 4.3.1 for welds previously without including plant-to-plant differences since welds irradiated in multiple plants were not included.

22 weld heats were analyzed that were irradiated in multiple plants, with at least three measurements per heat for a total of 155 TTS measurements. The source of this data included information outside of the E900-15 database, as the data descriptors in E900 made it difficult to determine heats which were identical. However, an effort was made to ensure that no duplicates from the E900 database and outside sources existed. The average error (residual bias) and  $\sigma$  were determined for each heat. The residuals were corrected for each heat bias and  $\sigma$  was calculated to be 19.5°F. This value is the  $\sigma$  for these heats which also includes the effect of plant differences and the inability of the ETC to adjust for temperature differences. The resulting uncertainty difference when using weld  $\sigma_{\text{heat}}$  with and without plant differences is shown in Equation 7.

**Equation 7**      *Weld Metal*  $\sigma_{\text{multiplant}} = \sqrt{19.5^{\circ}\text{F}^2 - 16.9^{\circ}\text{F}^2} = 9.7^{\circ}\text{F}$

The resulting effect of multiple plant irradiations for SRM and weld heats is slightly different (11.8°F for SRM plates vs. 9.7°F for welds). Since the SRM plates were irradiated in more plants than a typical RV weld material, it is not surprising that the SRM value is slightly higher. Additionally, typical RV materials would not be expected to be irradiated in as many plants as the SRM heats were irradiated in. A value of 11°F is recommended for use, as it is slightly above the average of the two  $\sigma_{\text{multiplant}}$  values. Therefore, when applying the heat-specific adjustment to an RPV different than the one in which all samples were irradiated, an uncertainty of  $\sigma_{\text{multiplant}} = 11^{\circ}\text{F}$  should be included in the margin term as shown in Equation 1 (Table 2-1). It is recommended that the 11°F of margin is considered whenever any data from another plant is included in the evaluation, even if data from the actual plant exists. This is considered acceptable, because the addition of 11°F in the margin term results in only a small change and addresses the larger scatter observed between plants as presented in this section.

## 5 REFERENCES

1. Kirk, M. and Erickson, M., "A Code Case Concerning the Effect of Embrittlement on Index Temperature Metrics," PVP2020-21185, Proceedings of the ASME 2020 Pressure Vessels & Piping Conference, 2020.
2. American Society of Mechanical Engineers (ASME) Boiler and Pressure Vessel Code Section XI, Division 1, "Rules for Inservice Inspection of Nuclear Power Plant Components."
3. U.S. Nuclear Regulatory Commission, Office of Nuclear Regulatory Research, Regulatory Guide 1.99, Revision 2, "Radiation Embrittlement of Reactor Vessel Materials," May 1988. [*Agencywide Documents Access and Management System (ADAMS) Accession Number ML003740284*].
4. Code of Federal Regulations, U.S. Nuclear Regulatory Commission, 10 CFR Part 50.61, "Fracture Toughness Requirements for Protection Against Pressurized Thermal Shock Events," 84 FR 65644, November 29, 2019.
5. ASTM E900-15, "Standard Guide for Predicting Radiation-Induced Transition Temperature Shift in Reactor Vessel Materials," ASTM International, 2015.
6. NRC Technical Letter Report TLR-RES/DE/CIB-2019-2, "Assessment of the Continued Adequacy of Revision 2 of Regulatory Guide 1.99," U.S. Nuclear Regulatory Commission, Office of Nuclear Regulatory Research, July 2019. [*ADAMS Accession Number ML19203A089*]
7. ASTM E185, "Standard Practice for Conducting Surveillance Tests for Light-Water Cooled Nuclear Power Reactor Vessels," American Society for Testing and Materials, All Versions.
8. "Adjunct for E900-15 Technical Basis for the Equation Used to Predict Radiation-Induced Transition Temperature Shift in Reactor Vessel Materials," ASTM International, Adjunct No. ADJE090015-EA, 2015.  
<https://www.astm.org/BOOKSTORE/ADJUNCT/ADJE090015-EA.htm>
9. U.S. NRC Regulatory Issue Summary (RIS) 2014-11, "Information on Licensing Applications for Fracture Toughness Requirements for Ferritic Reactor Coolant Pressure Boundary Components," October 2014. [*ADAMS Accession Number ML14149A165*]
10. NRC Technical Letter Report TLR-RES/DE/CIB-2013-01, "Evaluation of the Beltline Region for Nuclear Reactor Pressure Vessels," November 2014. [*ADAMS Accession No. ML14318A177*]

11. Westinghouse Report WCAP-15117, Revision 0, "Analysis of Capsule V and the Dosimeters from Capsules U and X from the Catawba Unit 1 Reactor Vessel Radiation Surveillance Program," October 1998.
12. Westinghouse Report WCAP-17896, Revision 0, "Analysis of Capsule X from the FirstEnergy Nuclear Operating Company Beaver Valley Unit 1 Reactor Vessel Radiation Surveillance Program," September 2014.
13. Westinghouse Report WCAP-18518-NP, Revision 0, "Analysis of Capsule U from the Watts Bar Unit 2 Reactor Vessel Radiation Surveillance Program," March 2020.
14. Kusmaul, K., Föhl, J., and Weissenberg, T., "Investigation of Materials from a Decommissioned Reactor Pressure Vessel – A Contribution to the Understanding of Irradiation Embrittlement," Effects of Radiation on Materials: 14th International Symposium, ASTM STP 1046, N. Packin, R. Stoller, and A. Kumar, Eds., American Society for Testing and Materials, Philadelphia, 1990, pp. 80-104.
15. Hall, B., Server, W., Rosier, B., and Hardin, T., "Comparison of Radiation Embrittlement Prediction Models to High Fluence U.S. Power Reactor Surveillance Data," Proceedings of the ASME 2013 Pressure Vessels and Piping Conference, PVP2013-97039, 2013.
16. NUREG-1475, Revision 1, U.S. Nuclear Regulatory Commission, "Applying Statistics," March 2011.
17. Code of Federal Regulations, U.S. Nuclear Regulatory Commission, 10 CFR Part 50.61a, "Alternate Fracture Toughness Requirements for Protection Against Pressurized Thermal Shock Events," 75 FR 72653, November 26, 2010.
18. NUREG-2163, "Technical Basis for Regulatory Guidance on the Alternate Pressurized Thermal Shock Rule," Kirk, M., U.S. NRC, September 2018.
19. Kirk, M. "Embrittlement Trend Forecasting using Nearest Neighbors – an Update," Presentation to ASTM E10.02 subcommittee, June 29, 2020.

## APPENDIX A METHODS CONSIDERED

In addition to the method described in the body of this report, a number of methods were considered for developing a method to account for heat-specific data in a generic ETC, including those based on the following:

- Regulatory Guide 1.99, Revision 2 (RG1.99R2)
- 10CFR50.61a
- JEAC4201
- Nearest neighbor
- Bayesian statistics
- Adjustment of E900 coefficients.

### A.1 REGULATORY GUIDE 1.99, REVISION 2

RG1.99R2 [3] suffers from a number of short-comings as described in the NRC's adequacy evaluation [6] including: a lower standard deviation than is evident in up-to-date collections of surveillance data, non-conservative predictions at high fluence for base metals, ineffective credibility criteria, and lack of guidance for credible data use. The method chosen, as described in Section 2 herein, takes some of the practices from RG1.99R2 and improves and updates them.

### A.2 10CFR50.61a

Regulatory Guidance for 10CFR50.61a [17] is described in NUREG-2163 [18]. NUREG-2163 spells out four different statistical checks to evaluate agreement of heat-specific surveillance data relative to the embrittlement trend curve (ETC) (in this case, the ETC codified in 10CFR50.61a). The checks include an identification of statistically significant differences of heat specific data from the ETC of the following types:

- A. Uniform offset from the ETC
- B. Different fluence trend (slope) from ETC
- C. Larger uncertainty than ETC
- D. Outlier(s) from ETC mean prediction

NUREG-2163 discusses possible reasons why a failure of the above criteria might occur with recommendations for investigation. However, NUREG-2163 is focused specifically on ensuring

that mean predictions using the ETC are conservative compared to heat-specific measurement data and not on using heat-specific data to alter the prediction.

The statistical criteria of NUREG-2163 do not generate many statistically significant failures, because a 1% statistical significance criteria is adopted, so in most cases the unmodified ETC is used. In the cases when there is a non-conservative failure, the remedy is as follows for each of the deviation types described previously:

- A. ETC is biased (offset) with a factor of the mean residual minus  $2.33\sigma_{ETC}/\sqrt{n}$
- B. Adjust to greater slope of surveillance data
- C. Not addressed in NUREG-2163
- D. An outlier with low fluence (< 10% of RPV fluence projection) is not considered relevant. For a high fluence outlier, the ETC should be adjusted to bound the data.

Since the Alternate Pressurized Thermal Shock Rule is a probabilistic analysis, the mean trend is used, and the uncertainty is built into the method. Therefore, an offset to compensate for non-conservative data is needed only to ensure the mean is compensated sufficiently to account for highly non-conservative data. The uncertainty term does not change since it is built into the underlying probabilistic code. Additionally, there is no provision for improvement of the mean prediction for a case where surveillance data demonstrates the ETC is overly conservative.

### A.3 JEAC4201

Japan Electric Association Code (JEAC) 4201-2013 has a very complicated ETC which requires prediction of microstructural evolution, particularly precipitate volume fraction by atom probe tomography. Use of the ETC is not practical for the ASME Code, but the procedure does allow a mean bias adjustment of the ETC to the mean surveillance data [1].

### A.4 NEAREST NEIGHBOR

Nearest neighbor (NN) is based on the simple premise that things that appear similar are likely similar. In other words, materials which have similar characteristics should behave in a similar manner. CRIEPI is evaluating this methodology [19]. Currently, any materials in the database which have similar Cu, Ni, and irradiation temperature to the material of interest are considered to behave in a similar manner since Cu, Ni, and temperature have the largest effect on TTS. Phoenix Engineering Associates, Inc. (PEAI) found that NN follows local trends in data-dense regions but had some deviation in data-sparse regions. To date NN shows no strong evidence that  $\sigma$  (standard deviation) could be reduced.

One difficulty in NN application would be maintenance of a safety-related quality assured database from which to pull NN data. The NN method also cannot be used to reduce  $\sigma$  for heat-specific evaluation since the NN method includes uncertainty from differences between heats since multiple different heats are used to make a prediction.

## **A.5 BAYESIAN STATISTICS**

Bayesian statistics is a theory in the field of statistics where a degree of belief in an event is represented by the probability. One drawback of this method is that credit could not be taken for increased knowledge of actual measured data from a single heat since the sample size is small compared to the E900-15 database. Additionally, this statistical method would be difficult to implement.

## **A.6 ADJUSTMENT OF ASTM E900-15 COEFFICIENTS**

Heat specific adjustments of E900 coefficients was considered; however, this method has significant drawbacks. In particular, it is not possible to know if the correct coefficients were adjusted. As a result, mechanistic insight in the E900 equation is lost, and this method would be similar to a “guess-and-check” until superior results are achieved. For this reason, adjustments or re-fits of the E900 coefficients and equations were not considered.